IEEE Access
Multidisciplinary : Rapid Review : Open Access Journal

Received 29 November 2022, accepted 7 January 2023, date of publication 16 January 2023, date of current version 8 February 2023.

Digital Object Identifier 10.1109/ACCESS.2023.3237250

SURVEY

Comparative Performance Analysis of PV Module Positions in a Solar PV Array Under Partial Shading Conditions

HICHAM OUFETTOUL[1,3], (Member, IEEE), NAJWA LAMDIHINE[1], SAAD MOTAHHIR[2], (Senior Member, IEEE), NASSIM LAMRINI[3], IBTIHAL AIT ABDELMOULA[3], (Graduate Student Member, IEEE), AND GHASSANE ANIBA[1], (Senior Member, IEEE)

[1]Mohammadia School of Engineers, Mohammed V University in Rabat, Rabat 10080, Morocco
[2]Ecole Nationale des Sciences Appliquées, Université sidi Mohamed Ben Abdellah, Fes, Morocco
[3]Institut de Recherche en Energie Solaire et Energies Nouvelles (IRESEN), Green Energy Park, Ben Guerir, Morocco

Corresponding author: Hicham Oufettoul (hichamoufettoul@research.emi.ac.ma)

This work was supported by INTELLIGENT PV Project through the Research Institute in Solar Energy and New Energies (IRESEN).

ABSTRACT The irradiation intensity is the primary catalyst for energy production in photovoltaic (PV) systems. Nevertheless, it alleviates partial shading (PS) by inhibiting power production, primarily in habitable metropolitan areas, owing to surrounding objects or high soiling rates, particularly in dry and semi-arid climates. Hence, the PV module's location, orientation, and tilt angle significantly affect its performance and shorten its durability. Thus, this study undertakes a benchmark analysis of the two distinct panel positions' performance using PSIM and MATLAB software simulations and an actual practical test. A visual inspection of a solar power plant in Morocco's Green Energy Park is the origin of the survey concept; it observes that the soil density consistently covers certain PV panel spots. In this context, the solar energy data of an intelligent home deployed in the earlier-mentioned research platform has been deployed to emulate the performance of future buildings challenged with various obstacles. Therefore, the roof-mounted PV system satisfied the home's energy demands. In the first scenario, the PV module is in portrait mode. In the second case, they are in landscape orientation. The findings of this investigation demonstrate that standard PV panels produce more power when arranged in a landscape configuration than in a portrait configuration, exhibiting a discrepancy of up to 1010 *Wh* for a modest PV system. Finally, this study suggests appropriate orientation and design recommendations for standard and advanced solar modules, mainly those deployed in arid and heavily populated urban regions featuring severe shading constraints.

INDEX TERMS PV system, photovoltaic module, reconfiguration, PV orientation, portrait, landscape, test-bed, partial shading, soiling effect.

I. INTRODUCTION

The world's skyrocketing energy needs, concern over pollution levels, and depletion of fossil fuels are hallmarks of the contemporary era, promoting the integration of renewable energies to tackle the issues mentioned earlier. However, their contribution to meeting the world's energy demands remains uncertain [1], [2]. Consequently, universities, governments, and industries have discovered several sustainable energy resources that can steer away from traditional sources. Moreover, accelerate the energy transition to clean resources that satisfy the energy requirements of multiple sectors, including logistics, supply chain operations, and power grid integration [3]. According to the International Energy Agency Renewables 2020 prediction study, renewable energy will account for 95 % of the newly installed power production by 2025. At the same time, solar energy will account for 60 % of all newly established renewable energy sources.

The associate editor coordinating the review of this manuscript and approving it for publication was Tarek H. M. EL-Fouly.

To date, global solar PV capacity addition is expected to reach approximately $160 \times 10^{9}\, W$ [4], [5]. Morocco is among the Middle East and North African (MENA) countries that receive tremendous solar irradiation, with around 3000 hours of sunlight per year and approximately 5000 $Wh/m^{2}/day$ of irradiation, especially during summer [6]. Moreover, the geographical location of Morocco makes it particularly appealing for solar, wind, and hydroelectric power production. Furthermore, it is among the African nations, involving a power transmission link to Europe. Therefore, it has attracted significant interest as a promising energy source by investing in its efforts and providing financial incentives to establish a gigantic renewable energy plant to fulfill its energy needs and international "Net Zero" targets by 2050 [7]. Unfortunately, most Moroccan territories experience harsh outdoor conditions, notably humidity, temperature, and high airborne dust rates [8]. Consequently, it suffers from dust deposition on the PV module surface. Hence, a photovoltaic system would deliver a relatively moderate power output because the soiling issue not only obstructs or scatters incoming irradiation but also absorbs heat, thus increasing the cell temperature. Indeed, the cells immediately positioned at the rear of the dust collection are severely damaged [9]. Sulaiman et al. conducted experiments demonstrating that dust deposited on a glass plate tilted at 45° inhibited transmissions by 18% and 30% on average after ten and 30 days, respectively [10]. Furthermore, Kichou et al.'s research indicated that the impact of pollution on the optical and electrical degradation of PV modules strongly depends on the technology utilized [11], [12], [13]. A recent study highlighted that the average yield degradation rates are 1.19 %, 1.17 %, and 1.67 % per year for polycrystalline, monocrystalline, and thin-film cadmium chloride, respectively [14]. Numerous experts have cited dust accumulation on PV panel glass as a primary concern [15]. Depending on the PV module orientation and tilt angle, they may spread evenly or irregularly across the solar module surface, collecting at the edges and corners [16], [17], [18]. Specifically, humidity, wind patterns, and the nature of dust vary according to the region's morphology, chemistry, and composition [19], [20], [21]. For instance, solar power plants in the MENA region differ from Nordic ones because deserts are the world's most outstanding mineral dust reserves. In 2014, Ghazi investigated global dust accumulation patterns and proved that the MENA region had substantial dust accumulation zones [22]. Chanchangi et al. investigated the correlation between climatic conditions, dust deposition, rebound, resuspension, and adverse effects on PV module performance [23]. As a consequence of aerosols absorbing moisture and gravitationally dropping onto surfaces, the above-described conditions promote dust settling on the PV modules. Furthermore, once the air is dry, the sand droplets transform into dust particles, generating a thin layer that covers the PV surface. Therefore, dust accumulation acts as a direct barrier to partial shading (PS) issues, representing a severe barrier to solar energy production. PS is a significant mismatch loss that may create hotspots owing to the uneven radiation exposure throughout the PV module [24]. As a result, shaded cells provide insufficient power and are constrained to flow the same current as units capable of producing high currents. Thus, the shaded units act as loads rather than generators, increasing the temperature and harming the PV array [25]. Moreover, statistical analysis demonstrated that the annual energy production reduction associated with shadows in residential applications ranged from 10% to 20% [26]. Besides, the shading effects on the edges and pillars waste approximately 18% to 35% of energy [27]. Hence, a regular and widespread practice to mitigate hotspot failure is to insert a bypass diode across a single cell or a set of cells to provide alternative flow paths for the current stemming from unshaded subgroup units. However, the reliability of bypass diodes is still being determined owing to scarce evidence, apart from infrequent experimental research on electrical and thermal characterization [28], [29], together assessing overlapping and nonoverlapping bypass diode topologies [30]. In addition, the multiple peaks in the power-voltage (P–V) curve make maximum power point tracking (MPPT) challenging. Therefore, although a strategy based on I-V characteristics may adequately explore PV array performance, it must typically explain the MPPT process [31], [32], [33]. Thus, the PS restriction distorts the related maximum power point (MPP) voltage using global maximum power point tracking methods [34], [35].

Similarly, cleaning is an effective strategy appended to the improved methodology list that removes impurities and extends the PV module's lifetime. However, the expense of such operations and proper planning are significant constraints [36], [37]. To obtain the best payback, PV system size, dusty climate, and seasonal sequence are critical considerations for establishing an optimal cleaning program. In this context. Extensive research has also addressed cleaning issues, including lists of methods and particle resuspension theories for assessing dust-cleaning procedures. The wind direction and velocity determine the dust distribution and removal from the PV module surfaces [38], [39]. Conventional use prefers interconnecting PV panels in a series-parallel (SP) topology to provide the required electrical parameters. Nevertheless, a solar PV plant may experience partial shading during operation, drastically lowering its power production. For this purpose, literature reviews have revealed several strategies for altering solar panel configurations, enhancing their efficiency, and mitigating shadowing effects [40]. The least obtrusive shading scenarios may be shown through experimentation with mathematical puzzles, unlike those inspired by classic approaches, such as Su-Do-Ku, Latin Square, and Magic Square [41], [42]. Considering the aforementioned studies in the literature. Figure 1 provides an overview of the techniques for enhancing the energy output of solar panels and their direct and indirect impacts on partial shadowing and dust buildup on the PV

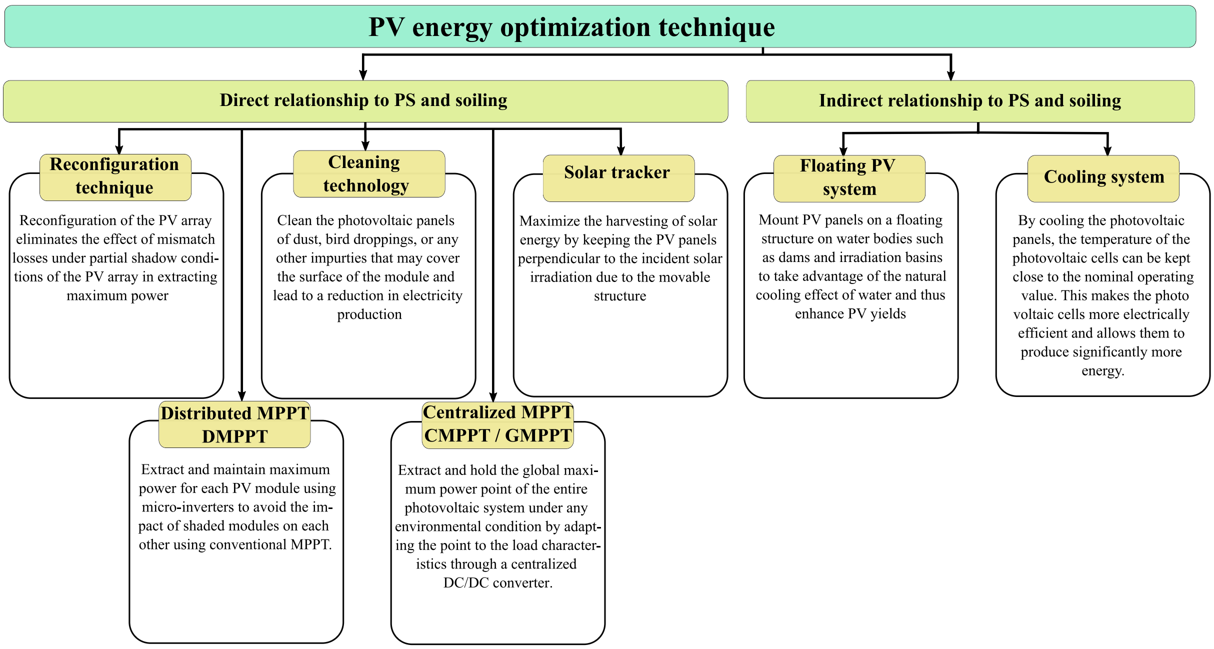

FIGURE 1. The most popular methods for increasing PV systems' outputs.

panel surface [43]. Ultimately, the framework aims to achieve an optimum solar panel arrangement for increased energy production under partial shade or in a dusty environment. The main contributions of this study are as follows: First, it sheds new light on PV systems in urban environments, including an unexpected increase in the number of buildings likely to cast shadows. Second, it urges researchers to redesign PV modules by rearranging the PV cells inside the PV modules in such a way as to remove the partial shading effect. Indeed, to reconsider the half-cut module and bifacial PV system. Third, the solar panels are rehabilitated in confined areas and rooftop spaces. Finally, we prioritize using machine-learning techniques to estimate and develop a PV reference model without requiring significant equipment.

A. PAPER ORGANIZATION

The rest of the paper is briefly organized as follows:

- The second section covers current solar cell modeling in the literature and demonstrates various PV panel interconnections.
- The third section is devoted to the simulation process to investigate the PV module behavior under uniform and non-uniform radiation distributions.
- The fourth section delves into the experimental methods for orientation situations using a 3D model and a PV array reference model description using an artificial neural network tool.
- Finally, a complete and concise finding, a discussion section, and a clearly stated conclusion outlining the merits and drawbacks of such PV orientations highlight prospective avenues for further research (see Figure 2).

II. EQUIVALENT CIRCUIT OF PHOTOVOLTAIC CELL

A photovoltaic (PV) cell, also called a solar cell, is a renewable energy technology that directly converts solar radiation into electricity by adopting the physical mechanism of the PV effect. The PV cell consists of two independent thin layers, each differently doped with electrons, and holes overloaded with semiconductor materials. Once the P-N junction is exposed to sunlight, it absorbs photon energy exceeding its bandgap energy to form barriers, namely electron-hole pairs [44]. In contrast, excess photon energy is converted to heat. Modeling PV cells is, thus, an indispensable step and a deciding factor in PV module simulation, granting an in-depth analysis of system management and the assessment of the temperature and irradiance impact on the panel's behavior. Various PV models, including implicit and explicit models, have been published and applied in the scientific literature to determine the current-voltage (I-V) and power–voltage (P-V) curves. However, explicit options require more computational work than implicit options, which require little computational effort [45]. Furthermore, they involve basic analytical formulas that provide researchers with a means to approximate the critical solar cell characteristics (Eq 1, 2, 3, and 4). As shown in Figure 3, the photovoltaic cell equivalent circuits most commonly cited in the literature are as follows (1D1R, 1D2R, 2D4R, 2D2R, 3D2R, 3D5R, and xD2R). Nevertheless, 1D2R (designated as a single-diode model) is the recommended option among the previously stated PV diode variants [46], [47]. Consequently, the current study selected a single-diode model because of its simplicity, conceptual ease, and a few vital components (IP V, Id, Rsh, Rs, and a2). The

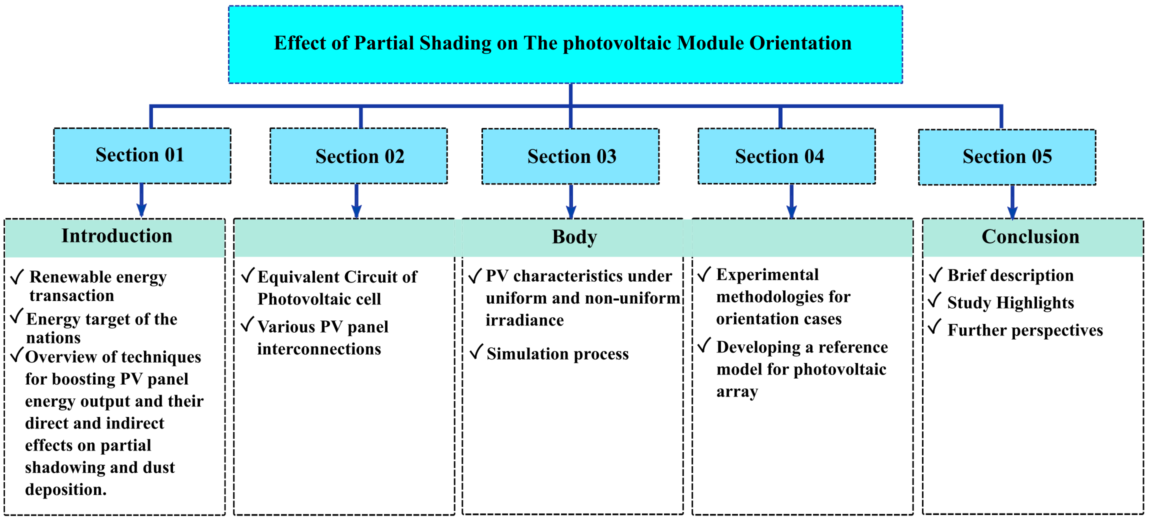

FIGURE 2. Paper organization.

equivalent circuit comprises a parallel-mounted diode with a shunt resistor to mimic a PN junction. It was then coupled with a series resistor to reflect the internal resistance of the PV cell (see Figure 3 (b)).

$$I_{PV} = I + I_d + I_{sh} \tag{1}$$

$$I_{PV} = (I_{sh} + \alpha(T - 298.15)) * \frac{G}{1000} \tag{2}$$

$$I_S = \frac{I_{sh} + \alpha(T - 298.15)}{\exp(\frac{q(V_{oc}+\beta(T-298.15))}{KTN_s}) - 1} \tag{3}$$

$$I = I_{PV} - (\exp^{\frac{q(V+I.R_s)}{KTnN_s}} - 1)I_S - \frac{V + IR_s}{R_{sh}} \tag{4}$$

where

I_{PV} : Represents the photocurrent.,
I_d : Diode current.
I_{sh} : Represents the shorting current.
n : Ideality factor of the p-n junction.
α : The short-circuit current's temperature coefficient.
β : The open-circuit voltage's temperature coefficient.
V_{oc} : Represent open circuit voltage.
G : Represent solar radiation.
T : Panel's temperature.
q : Represent the charge of the electron.
K : Represent constant of Boltzmann.
R_{sh} : Shunt resistances.
R_s : Series resistances.

The PV module is made up of PV cell packages that are connected serially to increase the output voltage. The cells are grouped into subparts that are connected in parallel with the bypass diode. Therefore, panels in typical large-scale PV arrays may be configured in series, parallel, or a combination of both topologies. Several interconnection arrangements exist in the literature, including (S, P, SP, HC, BL, TCT, and forced TCT, as well as hybrid topologies such as (SP-TCT, BL-TCT, and BL-H). Figure 4 illustrates basic topologies [48], [49].

TABLE 1. Almaden SEA P72T polycrystalline PV panel characteristics at STC.

Characteristics	Values
P_{max} Maximum Power	325 W
V_{mpp} Voltage at Maximum Power	37.64 V
I_{mpp} Current at Maximum Power	8.64 A
V_{oc} Open Circuit Voltage	46.12 V
I_{sc}Short Circuit Current	9.06 A
Weight (kg)	2.4 kg
Dimention (m)	$1.980 \times 0.99 \times 0.005$
Number of Cells	72

III. SOLAR RADIATION DISTRIBUTION EFFECT

A. PV CHARACTERISTICS UNDER UNIFORM IRRADIANCE

The commercial PV module considered in this subsection is a standard Almaden PV panel comprising 72 cells connected in series and arranged on three substrates, each of which has 24 units. The module's cell connectivity layouts are shown in Figure 5. The Almaden SEA P72T polycrystalline panel used in this research is mounted on the test bench. Figure 6 depicts the P-V and I-V curves of the PV module under different levels of homogeneous irradiation, ranging from 200 W/m^2 to 1000 W/m^2. Table 1 describes the characteristics of the module under standard test conditions (STC).

B. PV CHARACTERISTICS UNDER PS CONDITIONS AND THE SIMULATION PROCEDURE

Photovoltaic panels behave as loads rather than energy sources when temporarily or permanently darkened by dust or partial shading. Consequently, long-term shading could lead to destruction. As a remedy, the current of the unshaded cells is routed via an antiparallel mounted bypass diode in each cell subarray, preventing the overheating of the

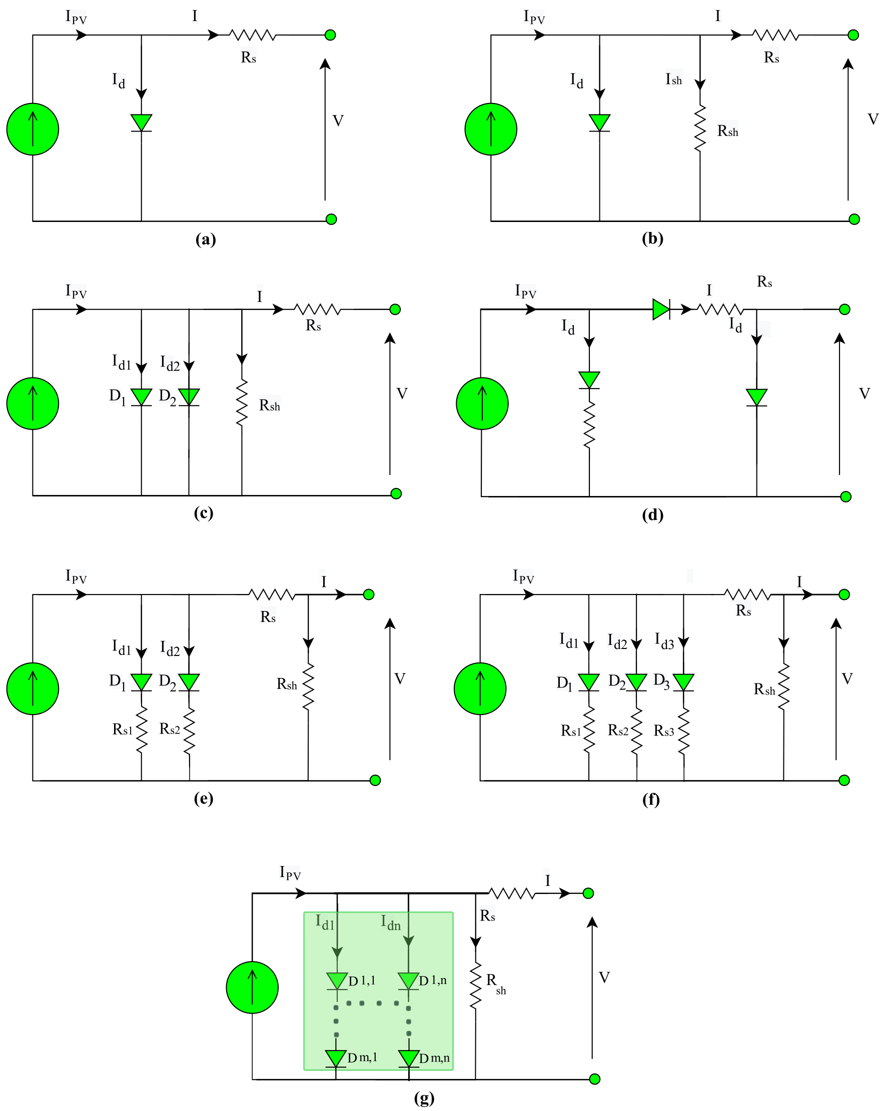

FIGURE 3. The most common PV cell's equivalent circuit in the literature.

uncovered cells [50]. In addition, the P-V curve exhibits multiple peaks during the bypass diode activation, where the global peak corresponds to the highest power produced. As part of the simulation process, the electrical characteristics are measured while evaluating the recommended landscape and portrait modes of PV panels under extreme soiling and shading conditions using a single diode model designed in the PSIM software. In the first shaded case, the PV module is mounted in portrait orientation and receives 1000 W/m^2 of irradiation. In contrast, the shaded cells absorbed 200 W/m^2, as shown in Figure 7. Similarly, the second shading scenario necessitates mounting the solar panel in landscape orientation. Furthermore, the shaded cells underneath received 200 W/m^2 irradiation. In contrast, unshaded cells are subjected to 1000 W/m^2 of irradiation. Figures 8 and 9 show the simulation of cell shading on the underside of the PV modules mounted in the landscape orientation. In addition, the Figure 7 depicts the cell-shading view at the bottom of the PV modules arranged in portrait orientation.

Consequently, these actions occasionally occur at the Green Power Park research platform. For instance, Figure 10 highlights the dust deposition on the PV module surface, including wet and dry accumulations. Furthermore, dust settles on the module's bottom surface owing to gravitational force and the panel frame capturing impurities. Likewise, Figure 11 shows the afternoon shadow cast from the first PV string on the remaining strings of an intelligent home built on the Green Energy Park research platform. The P-V curve showed a single peak under normal operating conditions, depending on the acquired results presented in Figure 6. Nevertheless, it produces several peaks owing to mismatched circumstances caused mainly by non-uniform irradiation. A limited current is produced by the darkened

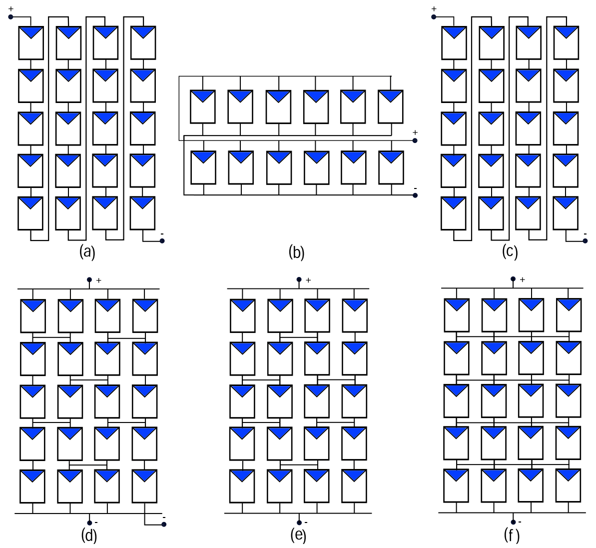

FIGURE 4. Basic topologies: (a) Total Cross-Tied, (b) Series, (c) Honey-Comb, (d) Bridge-Link, (e) Series-Parallel, and (f) Parallel.

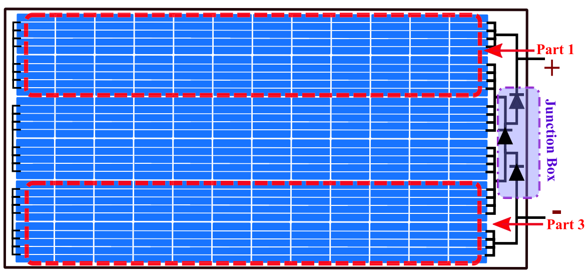

FIGURE 5. Standard PV Module Structure.

cells. Therefore, the current can freely circulate through illuminated cells without difficulty. However, the current produced by the well-lit cells is sufficient to harm the poorly lit cells, which mandates the alternative channel. The operating principle of the PV module and bypass diode behavior will drive our investigation regarding the scenarios mentioned above for the following explanation:

- **First Scenario:** This study adopts solar panels consisting of three cell clusters, represented by units called subparts cells, connected serially. The shading pattern applied at this instant covered only a single subpart, resulting in two peaks in the P-V curve, as shown in Figure (8 (c)). Each height corresponds to the power output level. The darkened sub-part corresponds to the local peak power. Therefore, it exhibited a mild current that could flow freely through the unshaded cells without enabling the bypass diode. Similarly, the voltage correlating to this current equals the sum of the subpart's voltages. Figure (8 (a)) emphasizes (in green) the paths of the current produced by the failing subpart cell. The Figure (8(b))
  Figure (8 (a)) emphasizes (in green) the paths of the current produced by the failing subpart cell. Figure (8 (b)) depicts the P-V curve of the shaded subparts, where the well-illuminated subfragment components generate a significant current that may induce irreparable damage to the shaded cells. Therefore, the bypass diode acts as an alternating current canal. Furthermore, the voltage proportional to the current generated by a well-lit subpart is the sum of the voltages omitted by the darker subpart. A red line in Figure (8 (a)) marks the current path. Besides, Figure (8 (b)) depicts the P-V curve of the lit subparts. Figure 9 illustrates the second pattern, wherein the partial shading mode is identical to the preceding stage. However, the global power peak is significantly lower than in the prior scenario, owing to the influence of the single irradiated subpart on the remaining two highly illuminated subparts.
- **Second Scenario:** In the second shading scenario, displayed in Figure 7, the shading is spread over the entire cell row underneath the PV module, reflecting the actual dust deposition and surrounding objects that undoubtedly provoke partial shading. Nevertheless, the power achieved is modest, and the resulting P-V curve incorporates a single peak, denoted as the panel that undergoes full shading. In addition, the mismatch among the subparts is non-existent, allowing the current to flow through the cells without enabling a bypass diode owing to the insufficient current. The green line indicates the current flow route. At the same time, Figure (7 (b)) represents the P-V curve of the PV module under partial shading conditions.

According to the simulation results of the two shading scenarios applied to a typical PV module, shading a single subpart in a landscape-mounting orientation led to almost one-third of the module's total power. Similarly, two-thirds of the module's overall capacity is lost when the two cell subparts are shaded. Thus, integrating practical MPPT metaheuristic algorithms is required to track the global maximum power point (GMPP) in such situations. In contrast, the second solar panel is mounted in portrait orientation. As a result, the shadow surrounding the module's footer cells causes the P-V curve to possess a single peak, delivering a maximum output power proportional to the full shading of the PV module. This results in a drastic decrease in power generation compared to the previous state. Typically, the MPPT strategy recommended for such circumstances is conventional MPPT.

IV. EXPERIMENTAL PROCEDURE

The experimental procedure of this investigation was to establish a photovoltaic array consisting of nine PV modules connected serially to meet the inverter's current and voltage requirements to support the simulation. Furthermore, it fulfills the daily energy requirements of an intelligent house; the experiment proceeds in two stages. The first step involves mounting the PV modules in portrait orientation for two

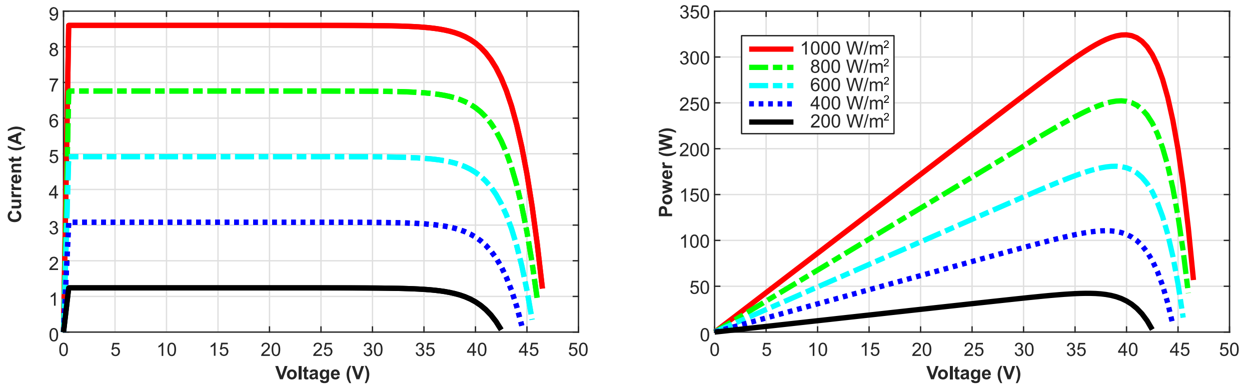

(a) (b)

FIGURE 6. I-V and P-V characteristics for different irradiation values.

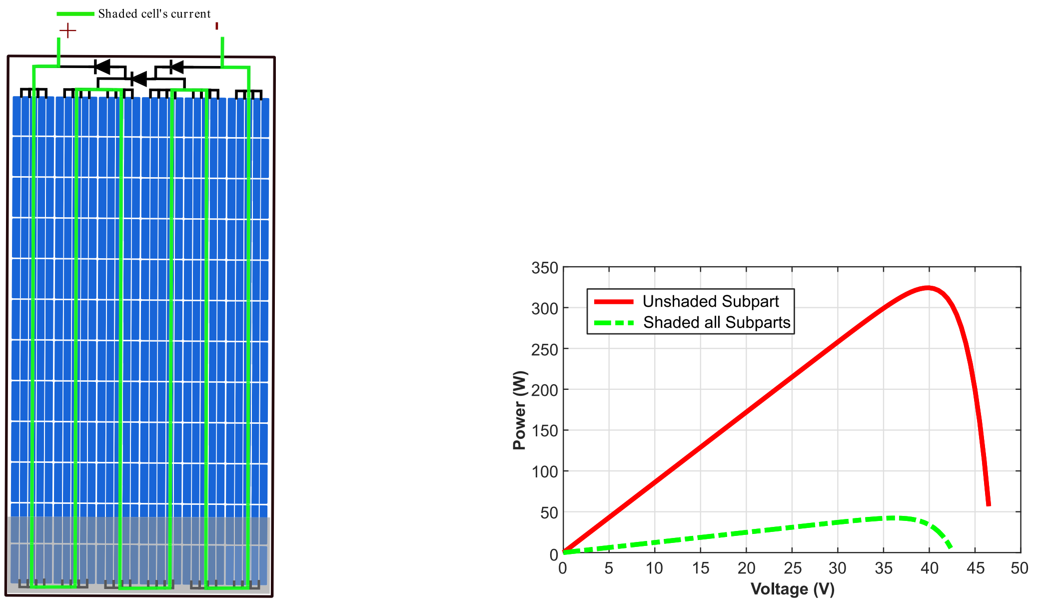

(a) (b)

FIGURE 7. Simulation of PV module underside cell shading mounted in the portrait mode. (a) View of the shaded PV module mounted in portrait orientation, and (b) The resultant P-V curve in portrait orientation.

months, starting on November 7, 2021, and ending on January 2, 2022. After that, the modules will operate in landscape orientation starting January 3, 2022. The overall capacity of the considered PV system is 3000 W. Table 2 lists their technical and mechanical characteristics. Figure 12 presents an overview of the test bed architecture. Eventually, the PV modules are installed in both orientations to ensure proper alignment. Furthermore, as previously mentioned, the test coincides with the solstice period, when the sun's path is at its lowest position. Consequently, the shade afforded by the strings is crucial, particularly in tiny metropolitan areas.

The soiling issue is also included indirectly in the following section, as the shading covers premises identical to the soiling observed in solar units at the Green Power Park facility. Likewise, shading is transient, unlike soiling, which is permanent as long as specific prerequisites such as

TABLE 2. Technical characteristics of the studied PV systems.

Characteristics	Values
Installed PV power	3000 W
Number of modules	9
PV Technology	*Poly*
Module inclination	31°
Module orientation	*South*

precipitation are missing. Similarly, solar system architecture and sizing are extensively evaluated to determine the most delicate PV module placements. However, this geographical area occasionally experiences unusual wind speeds, which may destroy the modules on the rooftops of the buildings. Furthermore, authorized interspacing between strings is

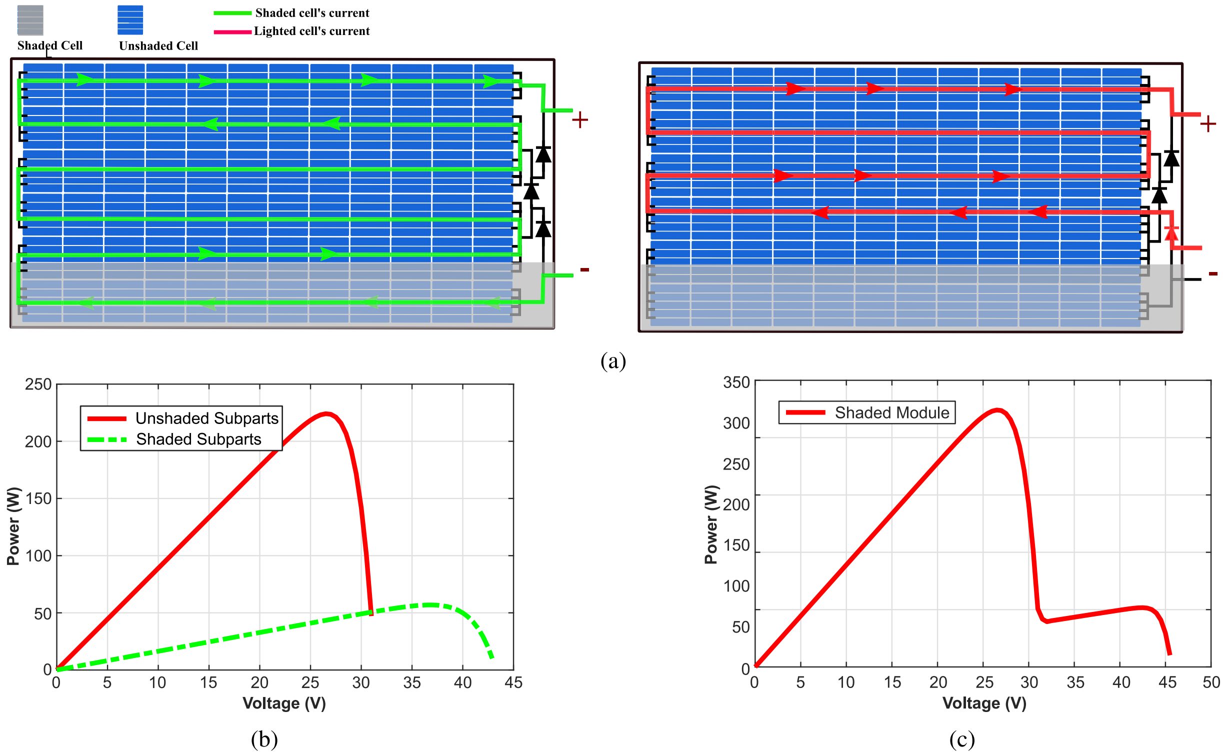

FIGURE 8. Simulation of the first shading case of landscape-mounted PV modules' underside cells. (a) View of the shaded PV module mounted in landscape mode, (b) The P-V explanatory curve of current, and (c) The resultant P-V curve in landscape orientation.

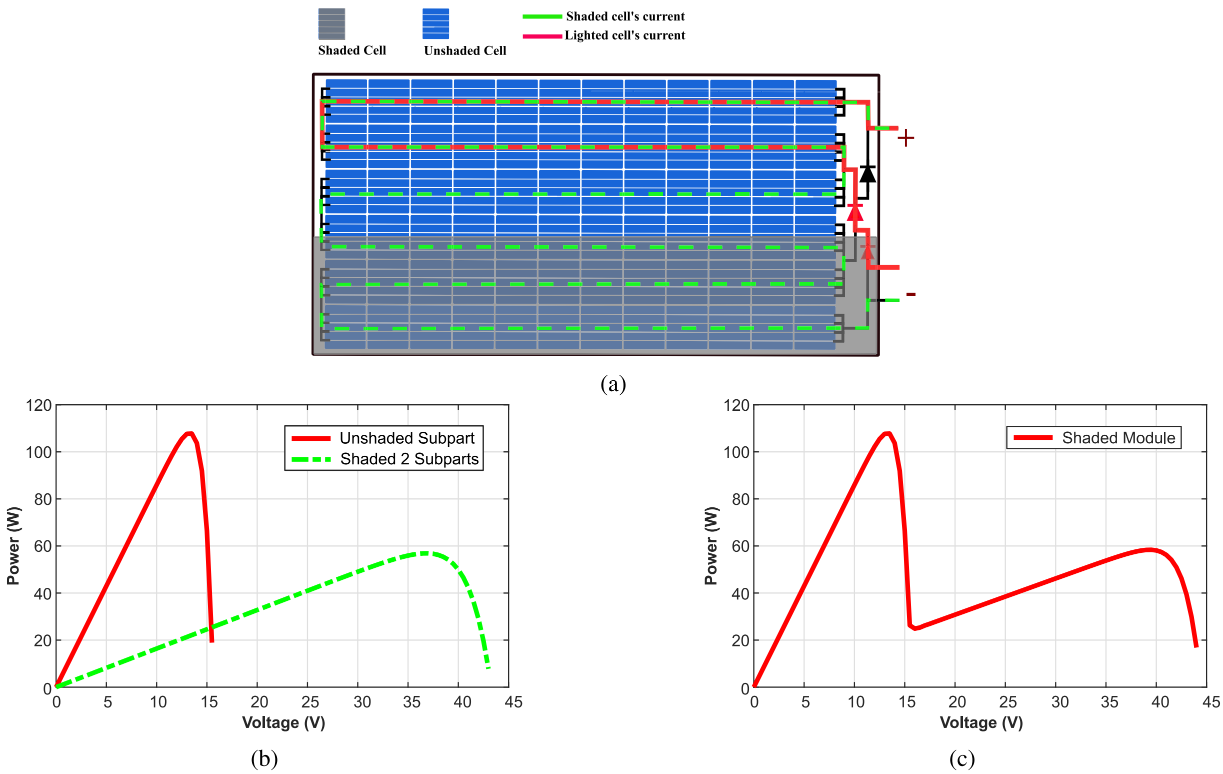

FIGURE 9. Simulation of the second shading case of landscape-mounted PV modules' underside cells. (a) View of the shaded PV module mounted in landscape mode, (b) The P-V explanatory curve of current, and (c) The resultant P-V curve in landscape orientation.

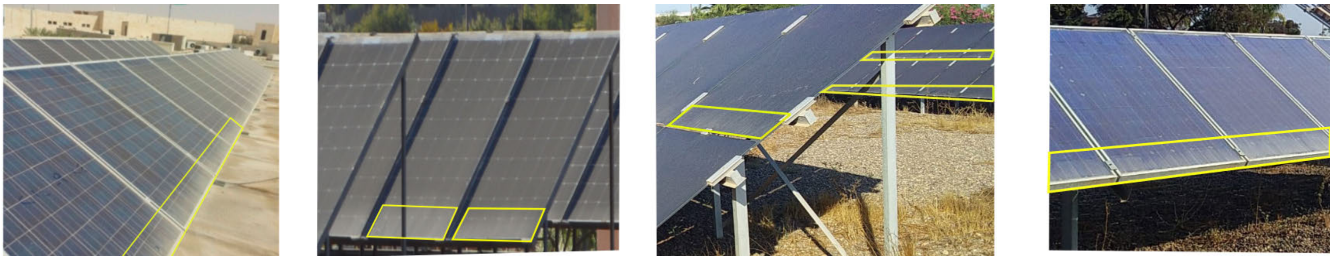

FIGURE 10. Soiling distribution on the Green Energy park's photovoltaic systems.

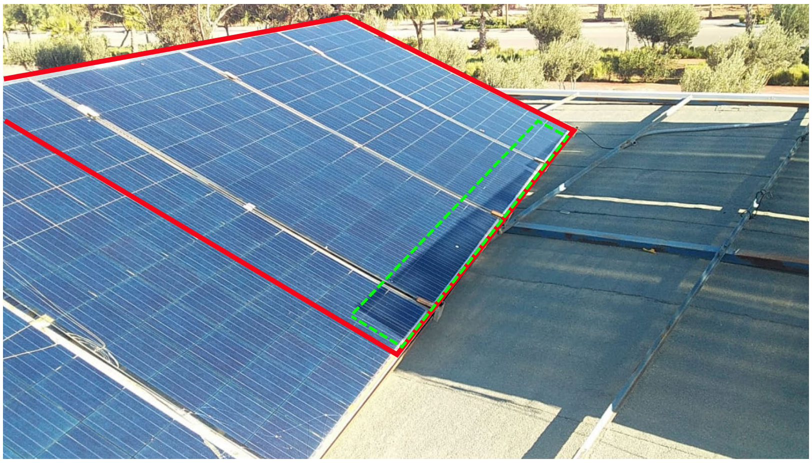

FIGURE 11. Shading of the photovoltaic string at Green Energy Park's test bench.

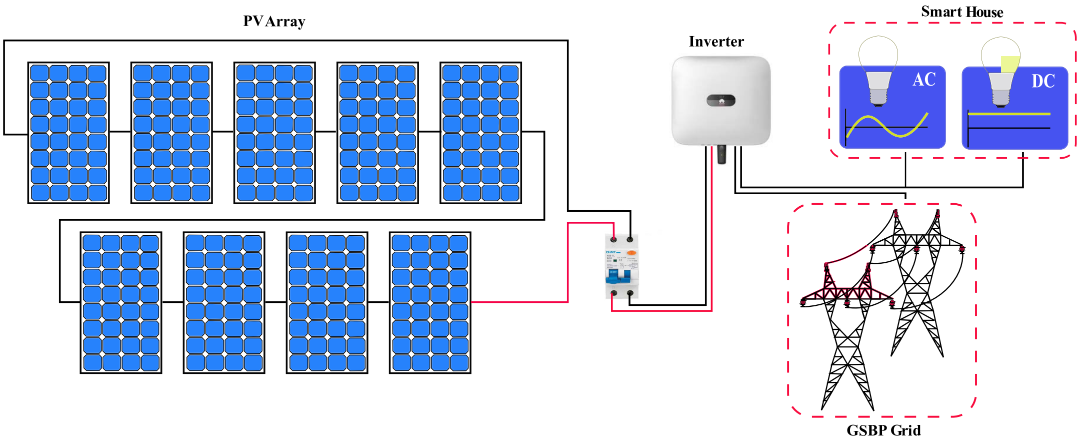

FIGURE 12. Electrical architecture of the test bench.

unrespected due to space challenges. The interspacing chosen for this case is appropriate based on preliminary 3D tests using sketch software, as shown in Figure 13.

A. EXPERIMENTAL SETUP FOR PORTRAIT ORIENTATION

In this scenario, the modules are arranged in portrait orientation, as shown in Figure 11. Four days are scheduled for display during data assignment. Namely, most days during this period are cloudy, and the designation of these days is neither random nor planned. Therefore, choosing such a date is unavoidable because of the relative insolation. Furthermore, the panels are adequately cleaned during testing to prevent further environmental effects and to focus exclusively on a single delimitation, bearing in mind that the evaluation depends on any fate that directly or indirectly induces shadowing on the photovoltaic cells within the same model. Figure 14 shows the power curves generated during the experimental period.

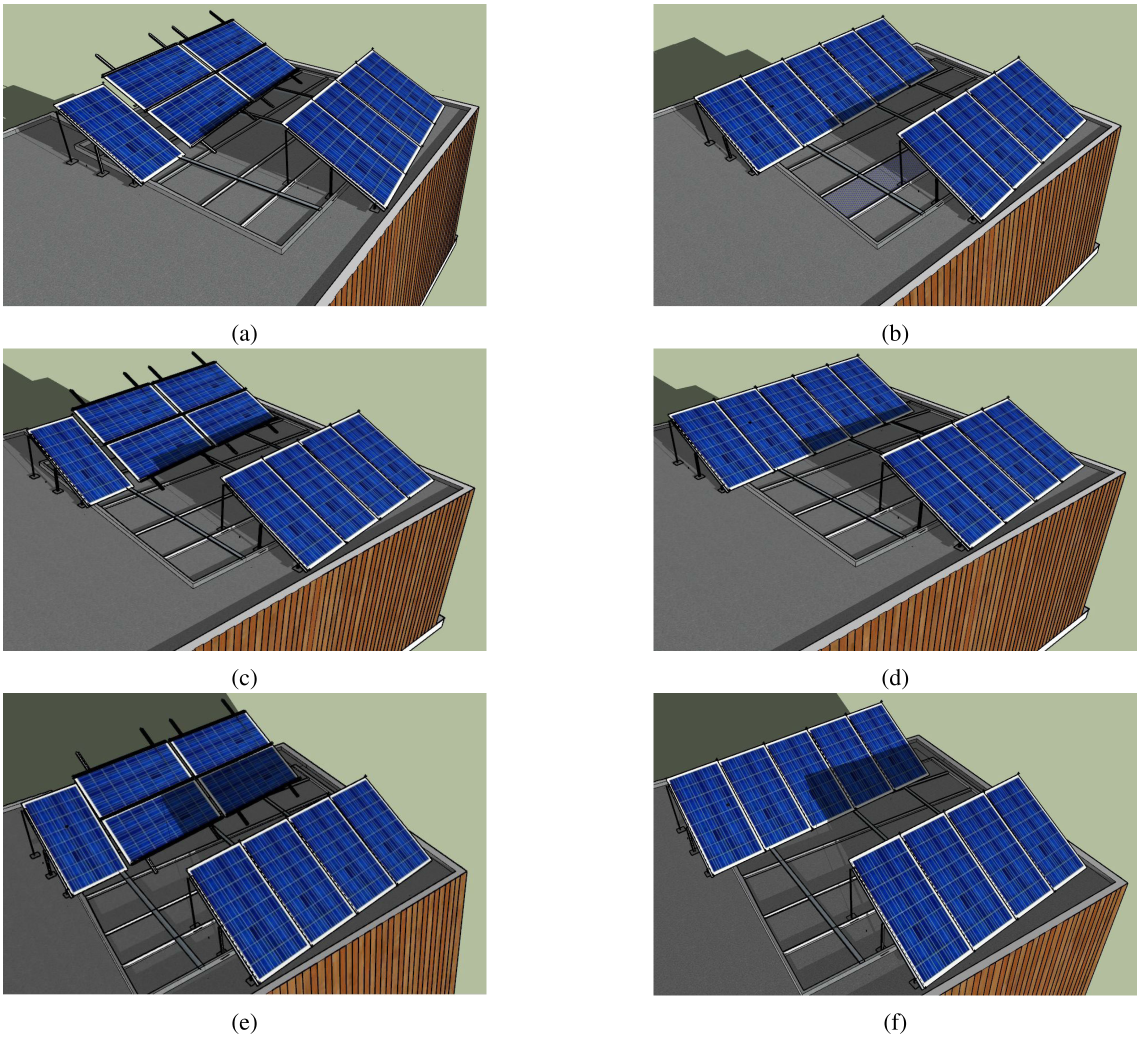

FIGURE 13. 3D view of the test bed under sketch software.

B. EXPERIMENTAL SETUP FOR LANDSCAPE ORIENTATION

The PV units that experienced shade exposure during the previous test are rearranged in landscape orientation, as depicted in Figure 15. Consequently, four days are allotted for examination, as previously performed for the portrait orientation trial. Hence, selecting these days has proven highly challenging. Moreover, the experiment is conducted at a specified time because the string's shadow appears most prominently when the sun's path is at its lowest point. Therefore, the changeover phase is identified as the solstice period. Figure 16 depicts the power output profiles of the PV plant.

C. REFERENCE MODEL DEVELOPMENT

To achieve a baseline model of the photovoltaic power plant considered in this framework, the performance of each scenario has been evaluated by comparing the power output for the instances mentioned earlier. Hence, the ANN model is applied with a certain degree of confidence to quantify the power profile generated by the photovoltaic power plant without experiencing mismatch failure. Also, the ANN model used several key performance metrics to figure out the recommended PV module position.

1) DATA ACQUISITION

The dataset utilized in this investigation spans the winter months of November 2021 to February 2022, during which significant temperature and solar irradiance fluctuations are anticipated. Figure 17 illustrates the test bench's electrical and meteorological data acquisition structures. At the same time, Figure 18 provides an aerial view of the electrical and meteorological station locations, which are close to 350 m. Thus, it may enhance the efficiency and accuracy of the ANN model.

2) DATA PRE-PROCESSING

Noise, missing values, and even inappropriate formats are standard features of real-world data that may or may not be directly relevant to an ANN model [51]. Therefore,

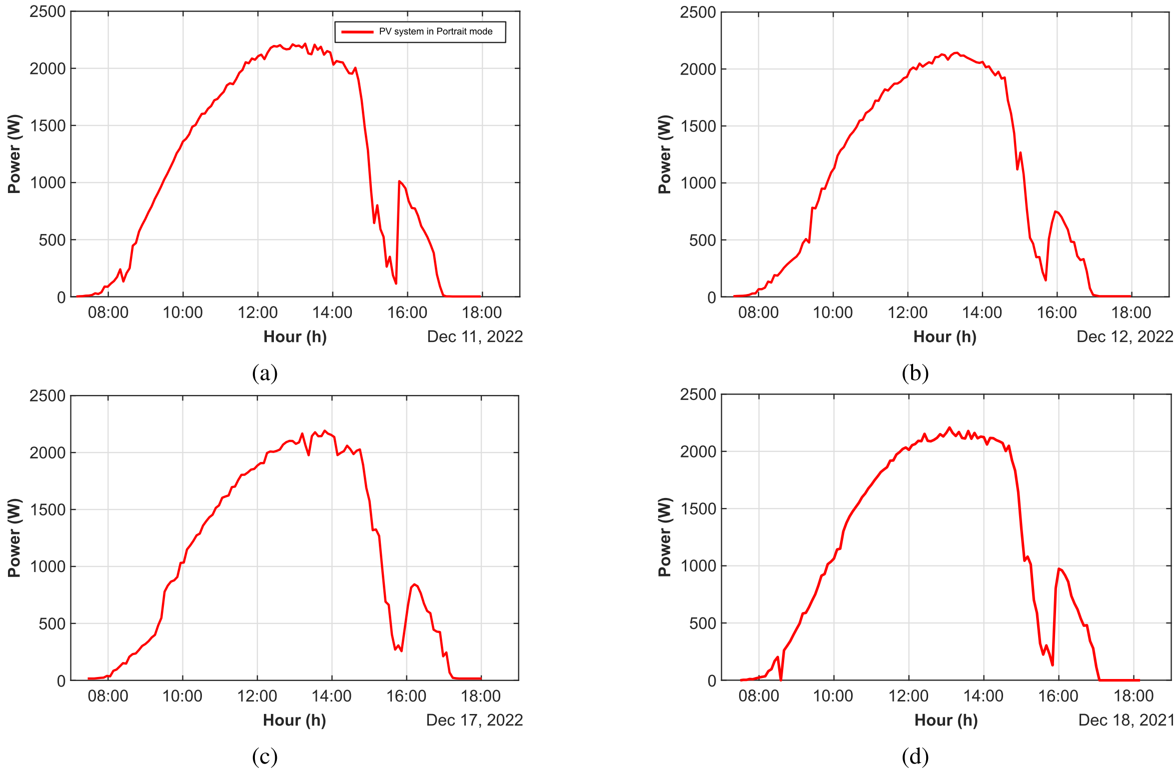

FIGURE 14. The power output of the photovoltaic system in portrait mode.

FIGURE 15. Second scenario of rearranging the PV module in landscape mode.

data preparation involves cleaning and restoring the data to acceptable requirements to enhance the accuracy and efficacy of the machine learning process. Although data preparation methodologies are readily available for the PV domain, they typically provide relatively generic procedures and concepts that require no in-depth understanding [52], [53]. Consequently, the first stage included resampling and synchronizing the data sources. The raw data is then filtered to identify and eliminate outliers before being replaced with nan values. Figure 19 shows the data preparation steps involved.

3) ARTIFICIAL NEURAL NETWORK MODEL

An artificial neural network (ANN) is a distributed parallel process acting as a single unit capable of sorting and processing information from experience. A neural network is analogous to the human brain in two aspects. First, the network learns from inputs during the process [54], [55]. Second, the information is recorded via synaptic weights, indicating the connection strength between the neurons. The neural network model used in this study included multilayered perceptrons. The input layer is the starting layer and includes various input variables. The final layer is the

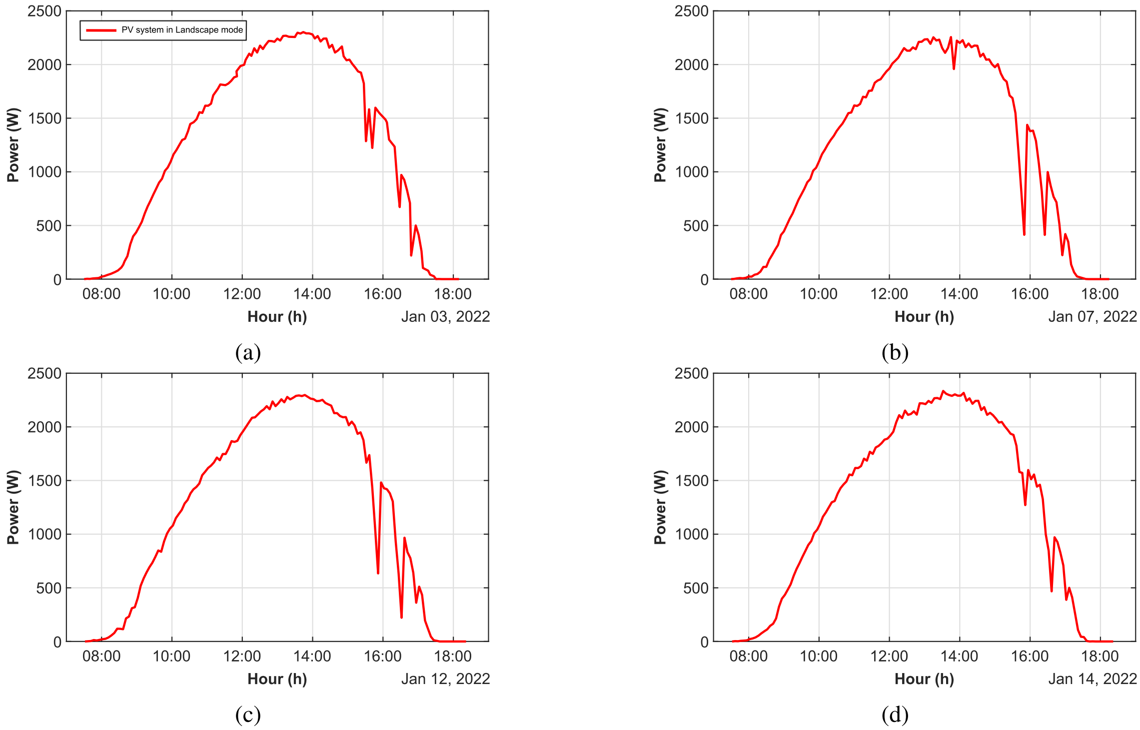

FIGURE 16. The power output of the photovoltaic system in landscape mode.

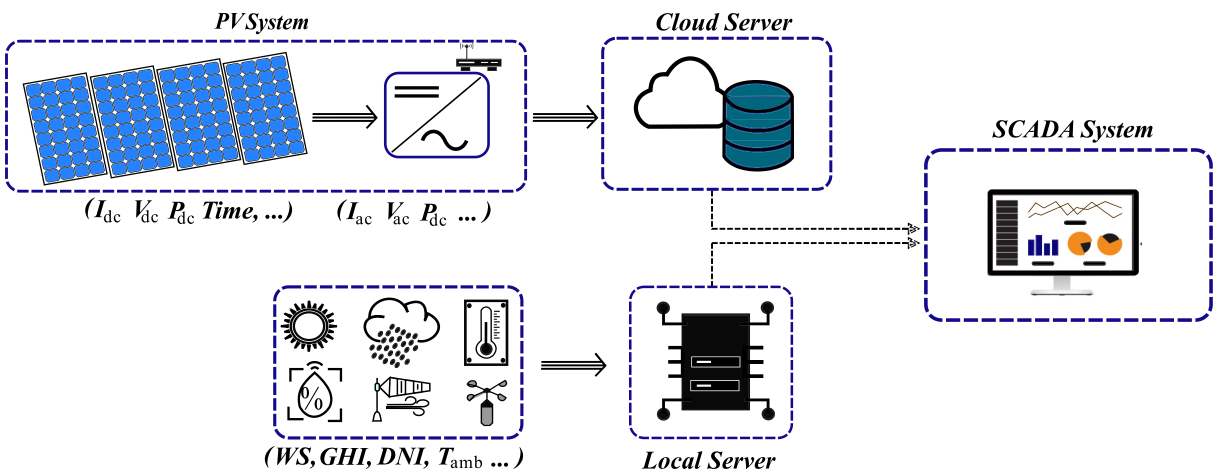

FIGURE 17. Test bench's electrical and meteorological data acquisition structure.

output layer that generates the expected results of the model. Multiple hidden layers between the levels interconnect the input and output layers. Once the training and test samples are established, a neural network design can be developed. The number of hidden layers and neurons in each input and hidden layer are the key attributes of ANN configurations. The selected ANN paradigm consisted of one input layer with ten neurons and two hidden layers with ten and five neurons, respectively. Thus, the root mean square error (RMSE), mean square error (MSE), and mean absolute error (MAE) are assessed to ascertain the optimal neural network model. The values are 0.096, 0.098, and 0.08, respectively. The figure illustrates the architecture of the ANN model. In addition, this project integrated a backpropagation (BP) algorithm to enhance learning. The BP has been identified as a robust supervised learning algorithm. Therefore, with an accuracy of 98.8%, the proposed ANN model is close to the reference model for both PV panel instances. Figures 21 and 22 show the results obtained when the ANN reference model is applied to test bed operation under trouble-free circumstances.

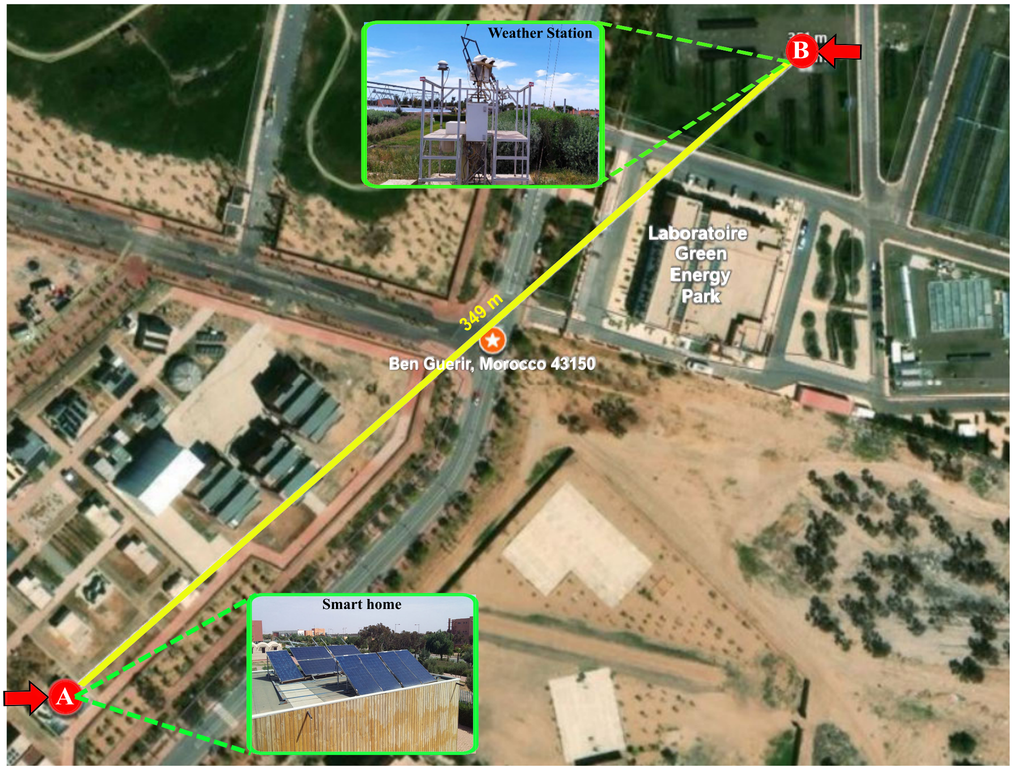

FIGURE 18. Aerial view of the electrical and meteorological station locations.

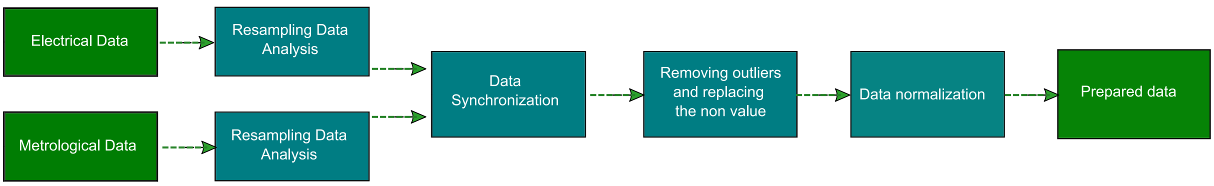

FIGURE 19. Data pre-processing stages.

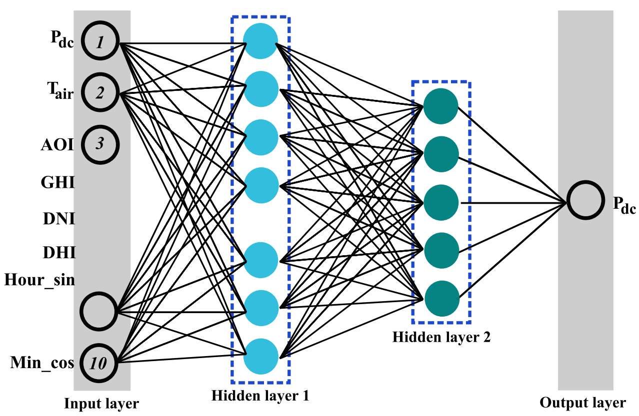

FIGURE 20. Architecture of the implemented ANN model.

D. RESULTS AND DISCUSSION

The analysis of the energy curves, modeling, and experimental results for the mounting orientation scenarios are presented in the following section. Besides applying key performance indicators, including energy production and loss, the results acquired for each orientation mode are compared to the ANN model's results. Thus, the current subsection summarizes the effective area influenced by the four module designs under the foot row shadow in both portrait and landscape modes. Finally, the "Appendix" section briefly summarizes the simulation results for all the PV orientations.

1) PORTRAIT ORIENTATION

The daily energy curves and bar graphs produced under shadowing demonstrate the energy profiles, as illustrated in Figure 23. This divulges a considerable fall in energy during the afternoon after the shade obscures the row footer of the PV panel. Under such conditions, the regular energy generated between 14 : 50 and 16 : 00 (hour) is significantly mitigated. For instance, the power generated on December 11, October 12, January 17, and January 18 are (733 *Wh* and

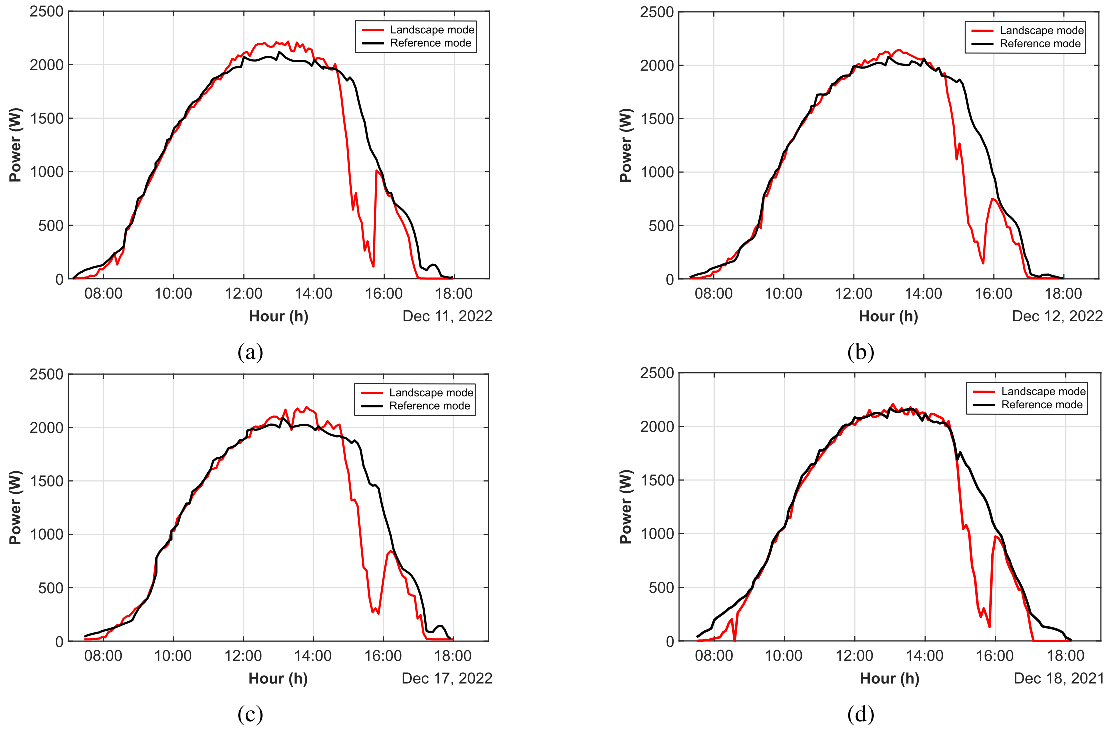

FIGURE 21. The estimated power of the PV array depending on the ANN model under trouble-free conditions.

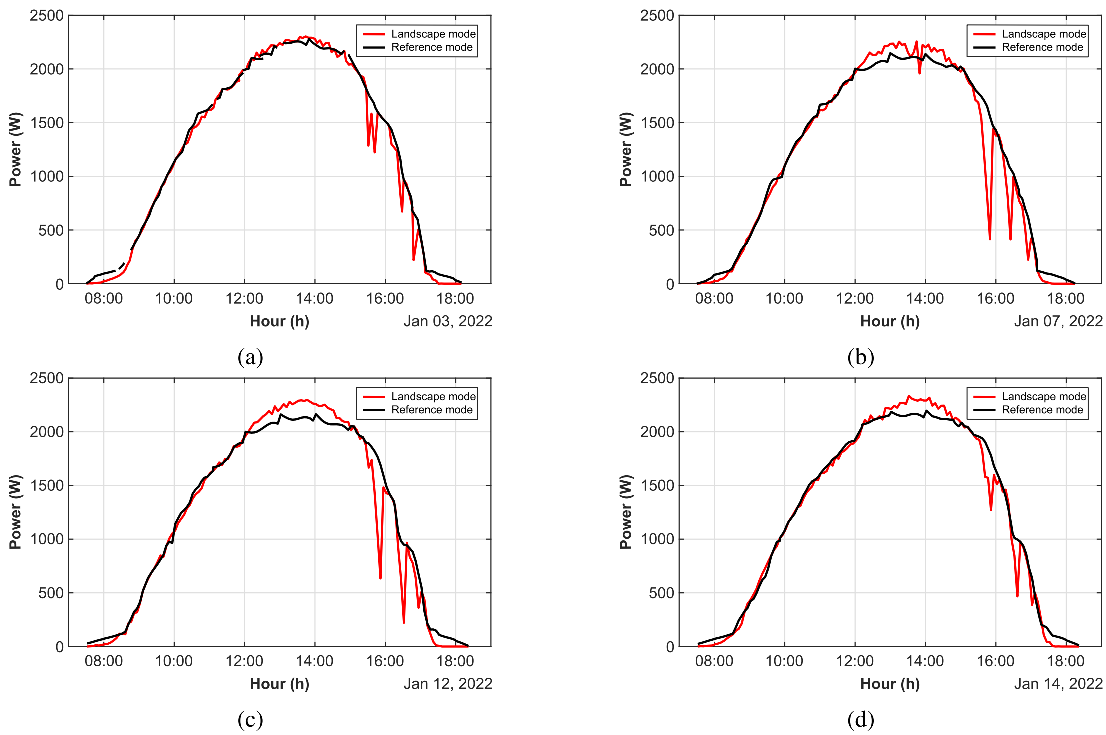

FIGURE 22. The estimated power of the PV array depending on the ANN model under trouble-free conditions.

590 *Wh*), (700 *Wh* and 490 *Wh*), (789 *Wh* and 593 *Wh*), and (694 *Wh* and 783 *Wh*) respectively. In contrast, the PV string emits much energy the hour before the establishment of the shadow, which may have a discernible explanation. Furthermore, the energy losses recounted on the dates mentioned earlier are 950 *Wh*, 1010 *Wh*, 987 *Wh*, and 870 *Wh*,

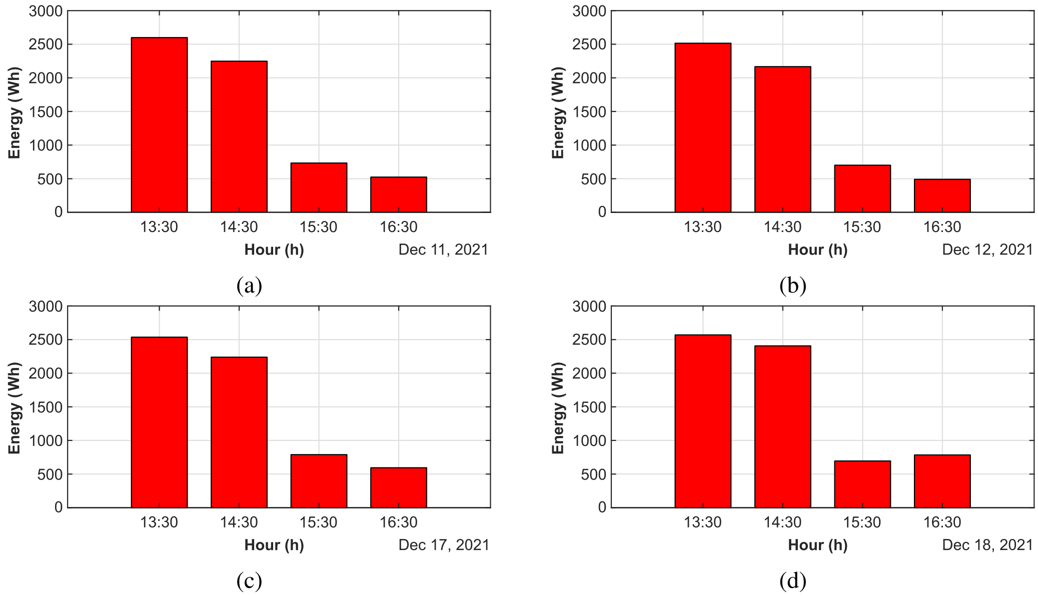

FIGURE 23. Graphic representation of the portrait orientation scenario.

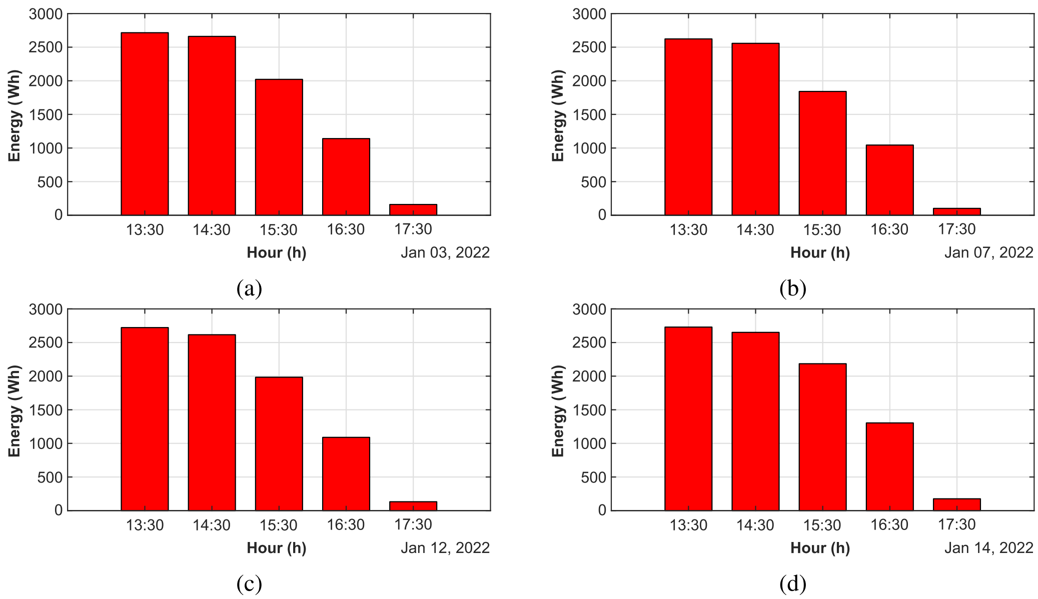

FIGURE 24. Graphic representation of the landscape orientation scenario.

respectively, as illustrated in Figure 25. Meanwhile, the following maximum power point voltages (216 V, 218 V, 213 V, and 217 V) were derived via a computation procedure utilizing the easy-to-implement GMPP model theory published by chalh at al. [56], once the system was undergoing a significant drop. To determine the voltage values associated with maximum power under the partial-shading effect (see Equations 5, 6, and 7) [56], [57]. In counterpoint, the voltages associated with the extracted power over a predisposing period are (266 V, 268 V, 281 V, and 259 V), respectively. Therefore, PV systems undoubtedly track the local maximum power point.

$$V_{mpp2} = N_s \times V_{mpp,STC} \tag{5}$$

$$V_{mpp1} = (N_s - N_{sh}) \times V_{mpp,STC} - N_{sh} \times 0.7 \tag{6}$$

$$V_{OC} = V_{OC,STC} \times K_v(T - T_{STC}) - a \times V_T \ln \frac{G}{G_{STC}} \tag{7}$$

2) LANDSCAPE ORIENTATION

The resorting daily energy curves and bar graph show the energy profile, shown in Figures 22 and 24, accompanied by significant growth in energy compared to the previous

TABLE 3. Graphic illustration of the effective area impacted by the shading effect of the row of cells underneath the four kinds of PV panel mounters in landscape orientation.

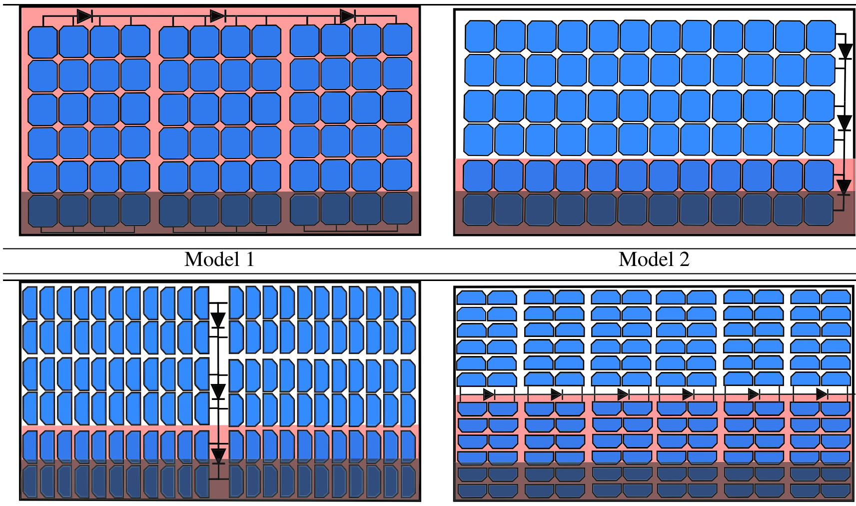

TABLE 4. Graphic illustration of the effective area impacted by the shading effect of the row of cells underneath the four kinds of PV panel mounters in portrait orientation.

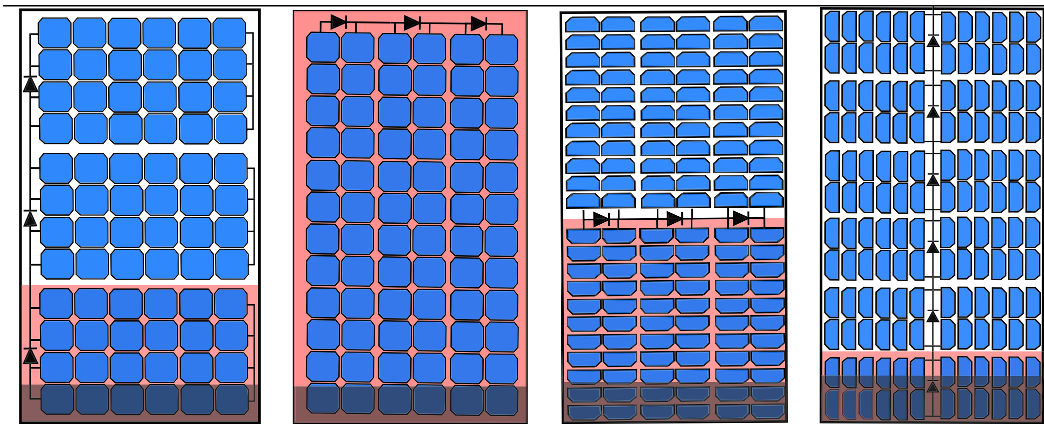

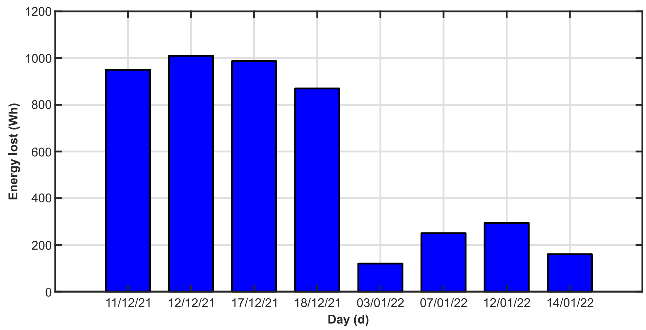

FIGURE 25. Graphical representation of energy lost.

scenario. Indeed, the energy produced between 14 : 50 and 16 : 00 (hour) is sufficient. For instance, the power produced on January 3, January 7, January 12, and January 14, respectively (2020 *Wh* and 1140 *Wh*), (1841 *Wh* and 1044 *Wh*), (1983 *Wh* and 1089 *Wh*), (2184 *Wh* and 1304 *Wh*)). Bayside, the reported energy loss on the aforesaid dates is 120 *Wh*, 250 *Wh*, 293 *Wh*, as seen in Figure 25. There is a limpid improvement in the amount of power lost in the landscape model case. During the period under consideration, the maximum power point voltage extracted is consistent with that acquired by performing a computation utilizing the easy-to-implement GMPP model theory, with some exceptions.

3) ANALYSIS

The extensive deliberation afforded by the power curve and bar chart has led the authors to highlight their impact on the performance of mounted panels in landscape orientation. The latter instance runs perfectly, addressing shadows, including those thrown on the PV panel's underside, dust deposition along the edge, and any other factors that may involve the formation of an anti-radiation layer on the PV panels. Furthermore, the power loss closely corresponds to the shaded area once the PV module foot is shaded. Unlike in portrait mode, when the PV panel beneath is obscured, the panel operates as fully shaded. Furthermore, the photovoltaic unit design successfully mitigated the shading consequences on power production, independent of the shadow source. This is shown by a series of simulations on different PV modules, including traditional and newer ones, as shown in Tables 3 and 4 (see appendix section).

V. CONCLUSION

In this contribution, the author introduces a theoretical, simulated, and concrete investigation of the different orientations of solar modules under partial shading and dust constraints. Furthermore, a simulation assignment is performed for conventional and advanced models to simulate the resulting energy required to ensure the injection of photovoltaic energy into new-generation power grids. This research focuses on photovoltaic installations located in areas with mandatory panel inclination and shading issues. This survey highlights certain main conclusions that can be summarized as follows:

- Identifying the orientation of the cell subparts is recommended as a preliminary step to properly mount the PV modules under partial shading and dust accumulation conditions.
- Improper orientation can lead to substantial energy losses exceeding 1000 *Wh* for a PV plant up to 3000 *W* when the PV panels are mounted in portrait mode.
- Advanced MPPT inverter technology may provide different energy loss rates than those indicated in this study; however, the landscape is significantly superior to the portrait mode.

Ultimately, this study introduces a perspective on the optimal PV panel mounting orientation, whereby the authors recommend using a landscape orientation based on the acquired results. The future of renewable energy will undoubtedly become everywhere to fulfill energy demands; hence, this research will serve as a powerful reference for scholars planning to conduct research in the MENA region or metropolitan areas. Furthermore, such research remains valid when the PV panel is tilted.

APPENDIX

See Tables 3 and 4.

ACKNOWLEDGMENT

The authors would like to convey their gratitude to the Green Energy Park research platform for the excellent work conditions and the convenience to use all necessitated measurement and test equipment.

REFERENCES

[1] N. Kannan and D. Vakeesan, "Solar energy for future world: A review," *Renew. Sustain. Energy Rev.*, vol. 62, pp. 1092–1105, Sep. 2016, doi: 10.1016/j.rser.2016.05.022.

[2] U. Bhattarai, T. Maraseni, and A. Apan, "Assay of renewable energy transition: A systematic literature review," *Sci. Total Environ.*, vol. 833, Aug. 2022, Art. no. 155159, doi: 10.1016/j.scitotenv.2022.155159.

[3] P. A. Østergaard, N. Duic, Y. Noorollahi, and S. A. Kalogirou, "Recent advances in renewable energy technology for the energy transition," *Renew. Energy*, vol. 179, pp. 877–884, Dec. 2021, doi: 10.1016/j.renene.2021.07.111.

[4] M. Hammoud, B. Shokr, A. Assi, J. Hallal, and P. Khoury, "Effect of dust cleaning on the enhancement of the power generation of a coastal PV-power plant at Zahrani Lebanon," *Sol. Energy*, vol. 184, pp. 195–201, May 2019, doi: 10.1016/j.solener.2019.04.005.

[5] O. E. Alani, M. Abraim, H. Ghennioui, A. Ghennioui, I. Ikenbi, and F.-E. Dahr, "Short term solar irradiance forecasting using sky images based on a hybrid CNN–MLP model," *Energy Rep.*, vol. 7, pp. 888–900, Nov. 2021, doi: 10.1016/j.egyr.2021.07.053.

[6] M. Boulakhbar, B. Lebrouhi, T. Kousksou, S. Smouh, A. Jamil, M. Maaroufi, and M. Zazi, "Towards a large-scale integration of renewable energies in Morocco," *J. Energy Storage*, vol. 32, Dec. 2020, Art. no. 101806, doi: 10.1016/j.est.2020.101806.

[7] M. Fasihi, D. Bogdanov, and C. Breyer, "Long-term hydrocarbon trade options for the Maghreb region and Europe—Renewable energy based synthetic fuels for a net zero emissions world," *Sustainability*, vol. 9, no. 2, p. 306, Feb. 2017, doi: 10.3390/su9020306.

[8] H. El-houari, A. Allouhi, S. Rehman, M. S. Buker, T. Kousksou, A. Jamil, and B. E. Amrani, "Design, simulation, and economic optimization of an off-grid photovoltaic system for rural electrification," *Energies*, vol. 12, no. 24, p. 4735, Dec. 2019, doi: 10.3390/en12244735.

[9] M. Abraim, H. E. Gallassi, O. E. Alani, H. Ghennioui, A. Ghennioui, N. Hanrieder, and S. Wilbert, "Comparative study of soiling effect on CSP and PV technologies under semi-arid climate in Morocco," *Sol. Energy Adv.*, vol. 2, Jan. 2022, Art. no. 100021, doi: 10.1016/j.seja.2022.100021.

[10] S. A. Sulaiman, H. H. Hussain, N. S. H. N. Leh, and M. S. I. Razali, "Effects of dust on the performance of PV panels," *Int. J. Mech. Mechatron. Eng.*, vol. 5, no. 10, pp. 2021–2026, Oct. 2011. Accessed: Jan. 8, 2023.

[11] S. Kichou, P. Wolf, S. Silvestre, and A. Chouder, "Analysis of the behaviour of cadmium telluride and crystalline silicon photovoltaic modules deployed outdoor under humid continental climate conditions," *Sol. Energy*, vol. 171, pp. 681–691, Sep. 2018, doi: 10.1016/j.solener.2018.07.028.

[12] J. Kim, M. Rabelo, S. P. Padi, H. Yousuf, E.-C. Cho, and J. Yi, "A review of the degradation of photovoltaic modules for life expectancy," *Energies*, vol. 14, no. 14, p. 4278, Jul. 2021, doi: 10.3390/en14144278.

[13] B. Laarabi, Y. E. Baqqal, N. Rajasekar, and A. Barhdadi, "Updated review on soiling of solar photovoltaic systems Morocco and India contributions," *J. Cleaner Prod.*, vol. 311, Aug. 2021, Art. no. 127608, doi: 10.1016/j.jclepro.2021.127608.

[14] R. Othman and T. M. Hatem, "Assessment of PV technologies outdoor performance and commercial software estimation in hot and dry climates," *J. Cleaner Prod.*, vol. 340, Mar. 2022, Art. no. 130819, doi: 10.1016/j.jclepro.2022.130819.

[15] R. Shenouda, M. S. Abd-Elhady, and H. A. Kandil, "A review of dust accumulation on PV panels in the MENA and the far east regions," *J. Eng. Appl. Sci.*, vol. 69, no. 1, pp. 1–29, Jan. 2022, doi: 10.1186/s44147-021-00052-6.

[16] E. Abdeen, M. Orabi, and E.-S. Hasaneen, "Optimum tilt angle for photovoltaic system in desert environment," *Sol. Energy*, vol. 155, pp. 267–280, Oct. 2017, doi: 10.1016/j.solener.2017.06.031.

[17] Y. A. Badamasi, S. Oodo, N. B. Gafai, and F. B. Ilyasu, "Effect of tilt angle and soiling on photovoltaic modules losses," in *Proc. 1st Int. Conf. Multidisciplinary Eng. Appl. Sci. (ICMEAS)*, Jul. 2021, pp. 1–5, doi: 10.1109/ICMEAS52683.2021.9692375.

[18] M. Chaabane, W. Charfi, H. Mhiri, and P. Bournot, "Performance evaluation of solar photovoltaic systems," *Int. J. Green Energy*, vol. 16, no. 14, pp. 1295–1303, Nov. 2019, doi: 10.1080/15435075.2019.1671405.

[19] W. Javed, B. Guo, B. Figgis, and B. Aïssa, "Dust potency in the context of solar photovoltaic (PV) soiling loss," *Sol. Energy*, vol. 220, pp. 1040–1052, May 2021, doi: 10.1016/j.solener.2021.04.015.

[20] M. A. M. Abdelsalam, F. F. Ahmad, A.-K. Hamid, C. Ghenai, O. Rejeb, M. Alchadirchy, W. Obaid, and M. E. Haj Assad, "Experimental study of the impact of dust on azimuth tracking solar PV in Sharjah," *Int. J. Electr. Comput. Eng.*, vol. 11, no. 5, p. 3671, Oct. 2021, doi: 10.11591/ijece.v11i5.pp3671-3681.

[21] Y. N. Chanchangi, A. Ghosh, S. Sundaram, and T. K. Mallick, "An analytical indoor experimental study on the effect of soiling on PV, focusing on dust properties and PV surface material," *Sol. Energy*, vol. 203, pp. 46–68, Jun. 2020, doi: 10.1016/j.solener.2020.03.089.

[22] S. Ghazi, A. Sayigh, and K. Ip, "Dust effect on flat surfaces—A review paper," *Renew. Sustain. Energy Rev.*, vol. 33, pp. 742–751, May 2014, doi: 10.1016/j.rser.2014.02.016.

[23] Y. N. Chanchangi, A. Ghosh, S. Sundaram, and T. K. Mallick, "Dust and PV performance in Nigeria: A review," *Renew. Sustain. Energy Rev.*, vol. 121, Apr. 2020, Art. no. 109704, doi: 10.1016/j.rser.2020.109704.

[24] Y.-Y. Hong and R. A. Pula, "Methods of photovoltaic fault detection and classification: A review," *Energy Rep.*, vol. 8, pp. 5898–5929, Nov. 2022, doi: 10.1016/j.egyr.2022.04.043.

[25] H. Oufettoul, S. Motahhir, G. Aniba, M. Masud, and M. A. AlZain, "Improved TCT topology for shaded photovoltaic arrays," *Energy Rep.*, vol. 8, pp. 5943–5956, Nov. 2022, doi: 10.1016/j.egyr.2022.04.042.

[26] M. R. Maghami, H. Hizam, C. Gomes, M. A. Radzi, M. I. Rezadad, and S. Hajighorbani, "Power loss due to soiling on solar panel: A review," *Renew. Sustain. Energy Rev.*, vol. 59, pp. 1307–1316, Jun. 2016, doi: 10.1016/j.rser.2016.01.044.

[27] W. Ma, M. Ma, H. Wang, Z. Zhang, R. Zhang, and J. Wang, "Shading fault detection method for household photovoltaic power stations based on inherent characteristics of monthly string current data mapping," *CSEE J. Power Energy Syst.*, early access, Aug. 18, 2022, doi: 10.17775/CSEEJPES.2021.09520.

[28] C. G. Lee, W. G. Shin, J. R. Lim, G. H. Kang, Y. C. Ju, H. M. Hwang, H. S. Chang, and S. W. Ko, "Analysis of electrical and thermal characteristics of PV array under mismatching conditions caused by partial shading and short circuit failure of bypass diodes," *Energy*, vol. 218, Mar. 2021, Art. no. 119480, doi: 10.1016/j.energy.2020.119480.

[29] R. Vieira, F. de Araújo, M. Dhimish, and M. Guerra, "A comprehensive review on bypass diode application on photovoltaic modules," *Energies*, vol. 13, no. 10, p. 2472, May 2020, doi: 10.3390/en13102472.

[30] S. Silvestre, A. Boronat, and A. Chouder, "Study of bypass diodes configuration on PV modules," *Appl. Energy*, vol. 86, no. 9, pp. 1632–1640, Sep. 2009, doi: 10.1016/j.apenergy.2009.01.020.

[31] H. Karmouni, M. Chouiekh, S. Motahhir, I. Dagal, H. Oufettoul, H. Qjidaa, and M. Sayyouri, "A novel MPPT algorithm based on Aquila optimizer under PSC and implementation using raspberry," in *Proc. 11th Int. Conf. Renew. Energy Res. Appl. (ICRERA)*, Sep. 2022, pp. 446–451, doi: 10.1109/ICRERA55966.2022.9922834.

[32] H. Oufettoul, G. Aniba, and S. Motahhir, "MPPT techniques investigation in photovoltaic system," in *Proc. 9th Int. Renew. Sustain. Energy Conf. (IRSEC)*, Nov. 2021, pp. 1–7, doi: 10.1109/IRSEC53969.2021.9741122.

[33] H. Rezk, M. Al-Oran, M. R. Gomaa, M. A. Tolba, A. Fathy, M. A. Abdelkareem, A. G. Olabi, and A. H. M. El-Sayed, "A novel statistical performance evaluation of most modern optimization-based global MPPT techniques for partially shaded PV system," *Renew. Sustain. Energy Rev.*, vol. 115, Nov. 2019, Art. no. 109372, doi: 10.1016/j.rser.2019.109372.

[34] H. Karmouni, M. Chouiekh, S. Motahhir, H. Qjidaa, M. O. Jamil, and M. Sayyouri, "Optimization and implementation of a photovoltaic pumping system using the sine–cosine algorithm," *Eng. Appl. Artif. Intell.*, vol. 114, Sep. 2022, Art. no. 105104, doi: 10.1016/j.engappai.2022.105104.

[35] F. Fitriyah, M. Z. Efendi, and F. D. Murdianto, "Modeling and simulation of MPPT ZETA converter using human psychology optimization algorithm under partial shading condition," in *Proc. Int. Electron. Symp. (IES)*, Sep. 2020, pp. 14–20, doi: 10.1109/IES50839.2020.9231890.

[36] K. Ilse, L. Micheli, B. W. Figgis, K. Lange, D. Daßler, H. Hanifi, F. Wolfertstetter, V. Naumann, C. Hagendorf, R. Gottschalg, and J. Bagdahn, "Techno-economic assessment of soiling losses and mitigation strategies for solar power generation," *Joule*, vol. 3, no. 10, pp. 2303–2321, Oct. 2019, doi: 10.1016/j.joule.2019.08.019.

[37] P. M. Rodrigo, S. Gutiérrez, L. Micheli, E. F. Fernández, and F. M. Almonacid, "Optimum cleaning schedule of photovoltaic systems based on levelised cost of energy and case study in central Mexico," *Sol. Energy*, vol. 209, pp. 11–20, Oct. 2020, doi: 10.1016/j.solener.2020.08.074.

[38] A. Younis and M. Onsa, "A brief summary of cleaning operations and their effect on the photovoltaic performance in Africa and the middle east," *Energy Rep.*, vol. 8, pp. 2334–2347, Nov. 2022, doi: 10.1016/j.egyr.2022.01.155.

[39] B. Hammad, M. Al-Abed, A. Al-Ghandoor, A. Al-Sardeah, and A. Al-Bashir, "Modeling and analysis of dust and temperature effects on photovoltaic systems' performance and optimal cleaning frequency: Jordan case study," *Renew. Sustain. Energy Rev.*, vol. 82, pp. 2218–2234, Feb. 2018, doi: 10.1016/j.rser.2017.08.070.

[40] C. Li, Y. Yang, F. Fan, L. Xia, P. Peng, Y. Wang, K. Zhang, and H. Wei, "A novel methodology for partial shading diagnosis using the electrical parameters of photovoltaic strings," *IEEE J. Photovolt.*, vol. 12, no. 4, pp. 1027–1035, Jul. 2022, doi: 10.1109/JPHOTOV.2022.3173723.

[41] G. S. Krishna and T. Moger, "Reconfiguration strategies for reducing partial shading effects in photovoltaic arrays: State of the art," *Sol. Energy*, vol. 182, pp. 429–452, Apr. 2019, doi: 10.1016/j.solener.2019.02.057.

[42] R. Pachauri, S. Motahhir, A. K. Gupta, M. Sharma, A. F. Minai, M. S. Hossain, and A. Yassine, "Game theory based strategy to reconfigure PV module arrangements for achieving higher GMPP under PSCs: Experimental feasibility," *Energy Rep.*, vol. 8, pp. 10088–10112, Aug. 2022, doi: 10.1016/j.egyr.2022.08.006.

[43] A. E. Hammoumi, S. Chtita, S. Motahhir, and A. E. Ghzizal, "Solar PV energy: From material to use, and the most commonly used techniques to maximize the power output of PV systems: A focus on solar trackers and floating solar panels," *Energy Rep.*, vol. 8, pp. 11992–12010, Nov. 2022, doi: 10.1016/j.egyr.2022.09.054.

[44] A. S. Al-Ezzi and M. N. M. Ansari, "Photovoltaic solar cells: A review," *Appl. Syst. Innov.*, vol. 5, no. 4, p. 67, Jul. 2022, doi: 10.3390/asi5040067.

[45] M. Paludetto, E. Oroski, P. C. Stadzisz, C. H. da Costa, A. E. Lazzaretti, R. Linhares, and E. Rafae, "A MISO nonlinear model of photovoltaic panel based on system identification," in *Proc. IEEE PES Innov. Smart Grid Technol. Conf.-Latin Amer.*, Sep. 2019, pp. 1–6, doi: 10.1109/ISGT-LA.2019.8895325.

[46] R. Kumar and S. K. Singh, "Solar photovoltaic modeling and simulation: As a renewable energy solution," *Energy Rep.*, vol. 4, pp. 701–712, Nov. 2018, doi: 10.1016/j.egyr.2018.09.008.

[47] N. M. F. T. S. Araújo, F. J. P. Sousa, and F. B. Costa, "Equivalent models for photovoltaic cell—A review," *Revista Engenharia Térmica*, vol. 19, no. 2, p. 77, Dec. 2020, doi: 10.5380/reterm.v19i2.78625.

[48] A. M. Ajmal, T. Sudhakar Babu, V. K. Ramachandaramurthy, D. Yousri, and J. B. Ekanayake, "Static and dynamic reconfiguration approaches for mitigation of partial shading influence in photovoltaic arrays," *Sustain. Energy Technol. Assessments*, vol. 40, Aug. 2020, Art. no. 100738, doi: 10.1016/j.seta.2020.100738.

[49] D. Yousri, T. S. Babu, E. Beshr, M. B. Eteiba, and D. Allam, "A robust strategy based on marine predators algorithm for large scale photovoltaic array reconfiguration to mitigate the partial shading effect on the performance of PV system," *IEEE Access*, vol. 8, pp. 112407–112426, 2020, doi: 10.1109/ACCESS.2020.3000420.

[50] F. Harrou, B. Taghezouit, and Y. Sun, "Robust and flexible strategy for fault detection in grid-connected photovoltaic systems," *Energy Convers. Manage.*, vol. 180, pp. 1153–1166, Jan. 2019.

[51] J. F. Gaviria, G. Narváez, C. Guillen, L. F. Giraldo, and M. Bressan, "Machine learning in photovoltaic systems: A review," *Renew. Energy*, vol. 196, pp. 298–318, Aug. 2022, doi: 10.1016/j.renene.2022.06.105.

[52] A. Dairi, F. Harrou, Y. Sun, and S. Khadraoui, "Short-term forecasting of photovoltaic solar power production using variational auto-encoder driven deep learning approach," *Appl. Sci.*, vol. 10, no. 23, p. 8400, Nov. 2020, doi: 10.3390/app10238400.

[53] R. B. Roy, M. Rokonuzzaman, N. Amin, M. K. Mishu, S. Alahakoon, S. Rahman, N. Mithulananthan, K. S. Rahman, M. Shakeri, and J. Pasupuleti, "A comparative performance analysis of ANN algorithms for MPPT energy harvesting in solar PV system," *IEEE Access*, vol. 9, pp. 102137–102152, 2021, doi: 10.1109/ACCESS.2021.3096864.

[54] R. A. Rajagukguk, R. A. A. Ramadhan, and H.-J. Lee, "A review on deep learning models for forecasting time series data of solar irradiance and photovoltaic power," *Energies*, vol. 13, no. 24, p. 6623, Dec. 2020, doi: 10.3390/en13246623.

[55] L. Fara, A. Diaconu, D. Craciunescu, and S. Fara, "Forecasting of energy production for photovoltaic systems based on ARIMA and ANN advanced models," *Int. J. Photoenergy*, vol. 2021, pp. 1–19, Aug. 2021, doi: 10.1155/2021/6777488.

[56] A. Chalh, A. E. Hammoumi, S. Motahhir, A. E. Ghzizal, A. Derouich, M. Masud, and M. A. AlZain, ''Investigation of partial shading scenarios on a photovoltaic array's characteristics,'' *Electronics*, vol. 11, no. 1, p. 96, Dec. 2021, doi: 10.3390/electronics11010096.
[57] J. Gosumbonggot and G. Fujita, ''Partial shading detection and global maximum power point tracking algorithm for photovoltaic with the variation of irradiation and temperature,'' *Energies*, vol. 12, no. 2, p. 202, Jan. 2019, doi: 10.3390/en12020202.

HICHAM OUFETTOUL (Member, IEEE) received the bachelor's degree in renewable energy exploitation techniques from the Multidisciplinary Faculty of Ouarzazate, Morocco, in 2016, and the master's degree in renewable energy engineering, energy efficiency option network, and electrical energy from the Multidisciplinary Faculty of Beni Mellal, Morocco, in 2019. He is currently pursuing the Ph.D. degree with the Mohammadia School of Engineers, Rabat, Morocco. He was worked in the field of electrical and power engineering at the Taiyuan University of Technology, China. He is working on the IRESEN Project in collaboration with the CARTIF research platform to develop intelligent tools to improve the operation and maintenance of solar installations. His current research interests include intelligent reconfiguration techniques under partial shadowing effects, as well as the advanced detection and diagnosis of solar module failures.

NAJWA LAMDIHINE received the degree in electrical engineering, option: renewable energy from the National School of Applied Sciences (ENSA-Kenitra) Ibn Tofail University, Kenitra, Morocco, in 2015. She is currently pursuing the Ph.D. degree in electrical engineering with the Mohammadia School of Engineers, Mohammed V University of Rabat, Rabat, Morocco. Since 2018, she has been a Consultant in system engineering and operational safety with the Sector for the Stellantis Group, Casablanca, Morocco. Her research interests include the monitoring of photovoltaic solar installations and the detection and localization of defects in large-scale photovoltaic panels.

SAAD MOTAHHIR (Senior Member, IEEE) received the Engineering degree in embedded systems from ENSA, Fes, in 2014, and the Ph.D. degree in electrical engineering from SMBA University, in 2018. He has previous expertise in the industry as an Embedded System Engineer at Zodiac Aerospace Morocco, from 2014 to 2019. He has became a Professor at ENSA, SMBA University, Fes. He has published and contributed to numerous publications in different journals and conferences in the last few years, which are related to photovoltaic (PV) solar energy and embedded systems. In addition to this, he has published several patents at the Moroccan Office of Industrial and Commercial Property. He edited many books and acted as a guest editor of different special issues and topical collections. He is a reviewer and an editorial board of different journals. He was associated with more than 30 international conferences as a program committee/advisory board/review board member. He is a member of the Arab Youth Center Council. He is the ICDTA Chair Conference.

NASSIM LAMRINI received the Bachelor of Science degree in physical sciences and the Diploma degree in industrial engineering from the Faculty of Science and the National School of Applied Sciences, Mohamed First University, Oujda, Morocco, in 2017 and 2020, respectively, where he is currently pursuing the Ph.D. degree with the Laboratory for Smart Information and Communication Technologies, under the direction of Prof. El Mehdi Abdelmalek. He is currently working on the research platform Green Energy Park, Ben Guerir, Morocco, on the development of predictive maintenance approaches for photovoltaic plants, which aims to develop intelligent models able to diagnose and predict anomalies and under performance to improve the monitoring, operation, and maintenance of large-scale photovoltaic installations.

IBTIHAL AIT ABDELMOULA (Graduate Student Member, IEEE) received the degree in electrical engineering and embedded systems from the National School of Applied Science, Marrakesh, Morocco. She is currently pursuing the Ph.D. degree with the SIRC Laboratory, Hassania School of Public Works. She is currently an Electrical Engineer and the Head of the Digitalization and Data Science Group, Green Energy Park platform. She has experience in monitoring and supervising PV plants and the lead of the team behind the development of SCADA system of the Green Energy Park platform. She managed projects related to monitoring, big data analytics, and smart agriculture. Her area of research interests include supervision and anomaly detection in PV systems and the sizing and implementation of hybrid microgrids.

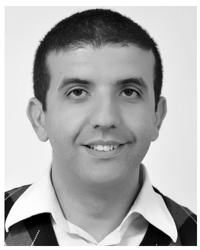

GHASSANE ANIBA (Senior Member, IEEE) received the Dipl.-Ing. degree in telecommunication engineering from the Institut National des Postes et Télécommunications (INPT), Rabat, Morocco, in 2002, and the Ph.D. degree in telecommunications from the Institut National de la Recherche Scientifique-Energy, Materials and Telecommunications (INRS-EMT), Montreal, Canada, in 2010. In 2010, after postdoctoral positions at the Université Laval, University of Ottawa, and King Abdullah University of Science and Technology (KAUST), he joined the Mohammadia School of Engineers (EMI), Rabat, where he is currently a Full Professor in electrical and telecommunication engineering. His current research interests include smart grids, cooperative distributed microgrids, traffic modeling in green cognitive networks, cooperative wireless networks, and wireless sensor networks. He was the TPC Co-Chair of the 3rd IEEE Middle East North Africa Communications Conference (MENACOMM 2020); the Co-Chair of the Special Session Smart Metering and Smart Homes at the 3rd IEEE Renewable Energies, Power Systems and Green Inclusive Economy (REPS GIE), in 2018; the Chairperson of the Smart and Green Systems and Networks track at the 19th IEEE Mediterranean Electrotechnical Conference (MELECON), in 2018; and the Chairperson of the cooperative techniques and relays session at the 20th International Conference on Telecommunications (ICT), in 2013. He is the Co-Principal Coordinator of the Institute for Research in Solar Energy and New Energies (IRESEN)—Green INNO-PROJECT titled: Intelligent Inspection of Photovoltaic Parks Using Aerial Images of Drones (2019–2023). Within the Erasmus+ Program of the European Union—Capacity Building in Higher Education, he was the Project Manager at EMI for the Project: AT-SGIRES—Advanced Teaching and Training on Smart Grid and Grid Integration of Renewable Energy Systems (2018–2021). In addition, he was the primary project coordinator within the International Research Projects CNR-CNRST (Morocco–Italy) for the Project: Cooperative Transmission Techniques for Smart Cities Data Sensing Collection (2016–2017). Finally, he was the Primary Coordinator of the IRESEN Project: MicroCSPs Contribution on the Management of an Electrical Grid including Renewable Energy Sources (2014–2018).